13 Theoretical Models for Duct Acoustic Propagation and Radiation

Lead author

Walter Eversman
University of Missouri-Rolla
Rolla, Missouri

Introduction

In the early history of jet propulsion the principal noise source was associated with the various mechanisms in the jet itself. Only in limited regions directly ahead of the engine and over limited operating conditions were noise-generating mechanisms related to the compressor important. The development of the turbofan engine, in which a significant portion of the thrust is derived from the fan stage, led to a reduction in jet noise and an increase in fan-compressor noise, thus exposing this source as one of major importance in the overall noise signature of the engine. In high-bypass-ratio turbofan engines the fan dominates the inlet-related noise, and thus we will refer to fan-compressor noise simply as fan noise.

Figure 1 shows the various noise sources in a turbofan engine and the general direction in which they are radiated. The fan is enclosed within a duct system and propagates noise upstream to be radiated from the inlet and downstream to be radiated from the fan exhaust. The acoustic system thus consists of the fan noise source, the ducts (which may be of nonuniform geometry and which may have acoustic treatment on the walls), and the exterior of the engine to which the acoustic field is radiated. The prediction of the radiated noise, and the design of the acoustic system to minimize this noise, must consider these elements. It is the purpose of this chapter to discuss techniques for the modeling of duct propagation and radiation. The source mechanisms are discussed elsewhere.

The fan duct in a typical turbofan engine, as shown in figure 1, consists of a more or less cylindrical inlet duct (which may have a centerbody) and an annular exhaust duct. Both the inlet and the exhaust duct are contoured for aerodynamic and propulsive efficiency. In modern engines there are no inlet guide vanes ahead of the fan, but there are struts or stators or both aft of the fan. The inlet duct and the exhaust duct have a length about the same or less than the inlet diameter. For

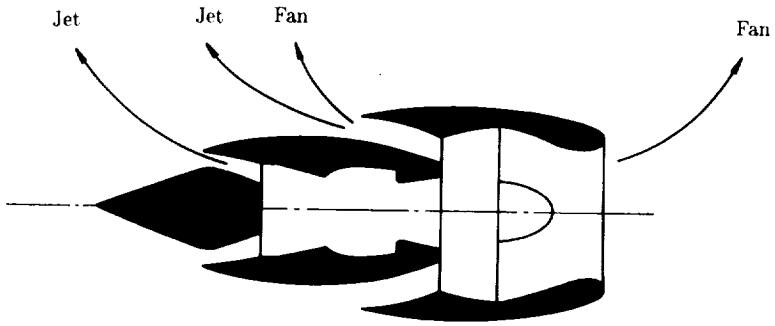

Figure 1. Major noise sources of turbofan engines.

noise suppression purposes acoustic treatment is installed on the duct walls in both the inlet and the exhaust duct, and in fact the treatment may cover most of the available surface. The aerodynamic flow through the ducts can cover a wide range of subsonic velocities, depending on the operating conditions of the engine. This flow in the ducts is nonuniform. The inlet and the exhaust duct radiate acoustic energy to free space through the nonuniform inlet aerodynamic flow field in the vicinity of the nacelle. The radiation process is coupled to the propagation process within the duct, so that in general the source and duct propagation and radiation should be considered simultaneously.

Except in the most advanced design and analysis procedures, the source model is considered to be independent of the propagation and radiation and is considered to be known, providing input to the duct propagation and radiation calculations. Furthermore, the duct propagation is generally considered independently of the radiation. Hence, in tracing the history of acoustic design and analysis methods for inlet suppression, it is found that the greatest emphasis has been on methods for the prediction of attenuation in acoustically treated ducts with a high-speed mean flow. Early work considered uniform ducts with uniform flow and was an extension of procedures developed for ducts with negligible mean flow, which had been of interest in connection with the acoustic design of air handling systems. It was soon recognized that the boundary layer in the mean flow at the duct wall can have a significant effect on the performance of acoustic treatment, so this phenomenon was added to the physical model and appropriate analysis methods developed. The question of duct nonuniformity, and the consequent nonuniformity in the mean flow, was then considered, and a substantial step in the extent of numerical analysis necessary was required.

The prediction of acoustic radiation from ducts can also be traced to investigations of air handling systems involving baffled and unbaffled pipes with negligible flow. Design and analysis requirements for turbofan engines have inspired some purely theoretical extensions of the early work by including the effect of an exhaust flow (applicable to the fan exhaust duct, although originally motivated by propagation through the jet). Approximation methods based on concepts of duct-mode propagation angles have been developed for the prediction of the direction in which peak radiation directivity occurs.

The development of computational methods in acoustics has led to the introduction of analysis and design procedures which model the turbofan inlet as a coupled

system, simultaneously modeling propagation and radiation in the presence of realistic internal and external flows. Such models are generally large, require substantial computer speed and capacity, and can be expected to be used in the final design stages, with the simpler models being used in the early design iterations.

In this chapter emphasis is given to practical modeling methods which have been applied to the acoustical design problem in turbofan engines. The mathematical model is established and the simplest case of propagation in a duct with hard walls is solved to introduce concepts and terminologies. An extensive overview is given of methods for the calculation of attenuation in uniform ducts with uniform flow and with sheared flow. Subsequent sections deal with numerical techniques which provide an integrated representation of duct propagation and near- and far-field radiation for realistic geometries and flight conditions.

A review of the status of duct acoustics in turbofan engines in reference 1 is extremely complete up to its 1975 publication date. In this chapter we unavoidably duplicate some of this discussion, with extensions representing advances since 1975. However, instead of an exhaustive review, we attempt to document specific design and analysis techniques of general utility.

The Acoustic Field Equations

In the following studies of duct acoustic propagation and radiation, modeling is based on linearization of the equations governing the isentropic motion of a nonviscous, non-heat-conducting perfect gas. The pertinent equations, in nondimensional form, are as follows:

Continuity :

$$\frac{\partial \rho^*}{\partial t} + \nabla \cdot (\rho^* \mathbf{V}^*) = 0 \tag{1}$$

Momentum :

$$\frac{\partial \mathbf{V}^*}{\partial t} + (\mathbf{V}^* \cdot \nabla)\mathbf{V}^* = -\frac{1}{\rho^*}\nabla p^* \tag{2}$$

Equation of State :

$$p^* = \frac{1}{\gamma}\rho^{*\gamma} \tag{3}$$

where the density ρ is scaled by ρ_r (a reference density), the velocity $\mathbf{V}$ is scaled by c_r (the reference speed of sound), pressure p is scaled by $\rho_r c_r^2$, time t is scaled by L/c_r (where L is a suitable reference length), and the spatial coordinates are scaled by L. In some applications a form of the energy equation is useful.

Energy :

$$\frac{\partial p^*}{\partial t} + \mathbf{V}^* \cdot \nabla p^* + \gamma p^* (\nabla \cdot \mathbf{V}^*) = 0 \tag{4}$$

The acoustic equations are obtained by considering small perturbations on a mean state ρ_o, p_o, and $\mathbf{V}_o$ so that

$$\rho^* = \rho_o + \rho$$

$$p^* = p_o + p$$

$$\mathbf{V}^* = \mathbf{V}_o + \mathbf{V}$$

The resulting acoustic field equations, after second-order and higher order terms in the small perturbations are ignored, are as follows:

Acoustic Continuity :

$$\frac{\partial \rho}{\partial t} + \nabla \cdot (\rho_o \mathbf{V} + \mathbf{V}_o \rho) = 0 \tag{5}$$

Acoustic Momentum :

$$\frac{\partial \mathbf{V}}{\partial t} + \mathbf{V}_o \cdot \nabla \mathbf{V} + \frac{1}{\rho_o} \nabla p + \mathbf{V} \cdot \nabla \mathbf{V}_o - \frac{1}{\gamma p_o \rho_o} p \nabla p_o = 0 \tag{6}$$

Acoustic Energy :

$$\frac{\partial p}{\partial t} + \mathbf{V}_o \cdot \nabla p + \mathbf{V} \cdot \nabla p_o + \gamma p_o (\nabla \cdot \mathbf{V}) + \gamma p (\nabla \cdot \mathbf{V}_o) = 0 \tag{7}$$

Acoustic Equation of State :

$$p = \gamma \frac{p_o}{\rho_o} \rho = c_o^2 \rho \tag{8}$$

In equation (8), c_o is the nondimensional local speed of sound in the mean flow.

In the acoustic radiation model the mean flow and the acoustic perturbations are taken as irrotational. In this case

$$\mathbf{V}^* = \nabla \Phi$$
$$\mathbf{V} = \nabla \phi$$
$$\mathbf{V}_o = \nabla \phi_o$$

where ϕ is the velocity potential nondimensionalized with respect to $c_r L$. The continuity and momentum equations and the equation of state are used in this case. The continuity equation follows directly from equation (5).

Acoustic Continuity Equation (Irrotational) :

$$\frac{\partial \rho}{\partial t} + \nabla \cdot (\rho_o \nabla \phi + \rho \nabla \phi_o) = 0 \tag{9}$$

In the case of the momentum equation, the implication of irrotationality is used ($\nabla \times \mathbf{V} = 0$), as is the isentropic equation of state ($dp^*/d\rho^* = (\rho^*)^{\gamma-1} = c^{*2}$), to obtain

$$\frac{\partial \mathbf{V}^*}{\partial t} + \frac{1}{2}\nabla(\mathbf{V}^* \cdot \mathbf{V}^*) + \nabla\frac{c^{*2}}{\gamma - 1} = 0$$

where c^* is the nondimensional local speed of sound. In terms of the velocity potential this can be written

$$c^{*2} = 1 - (\gamma - 1)\left[\frac{\partial \Phi}{\partial t} + \frac{1}{2}\left(\nabla\Phi \cdot \nabla\Phi - M_\infty^2\right)\right]$$

where the arbitrary function of time which arises is evaluated at infinity, where the reference conditions ρ_r and c_r are also defined. At infinity the nondimensional velocity is the Mach number M_∞. The nondimensional speed of sound c_∞^* is unity. Linearization yields the following isentropic relation for the mean flow:

$$c_o^2 = 1 - \frac{\gamma - 1}{2}\left(\nabla\phi_o \cdot \nabla\phi_o - M_\infty^2\right) \tag{10}$$

For the acoustic fluctuations, the following equation is used:

Acoustic Momentum Equation (Irrotational) :

$$\rho = -\frac{\rho_o}{c_o^2}\left(\frac{\partial \phi}{\partial t} + \nabla\phi_o \cdot \nabla\phi\right) \tag{11}$$

or

$$p = -\rho_o\left(\frac{\partial \phi}{\partial t} + \nabla\phi_o \cdot \nabla\phi\right) \tag{12}$$

In equations (11) and (12), ρ_o is the nondimensional local density and c_o is the nondimensional local speed of sound in the mean flow.

Propagation in Uniform Ducts With Hard Walls

In the case of a uniform duct with axially uniform mean flow, equations (5), (6), and (8) can be combined to yield the convected wave equation

$$\left(\frac{\partial}{\partial t} + M\frac{\partial}{\partial x}\right)^2 p = \nabla^2 p \tag{13}$$

The nondimensional velocity in this case is the local Mach number M and the nondimensional speed of sound is unity. This follows because of the nondimensionalization and because of the flow field uniformity. Equation (13) simplifies to the classic wave equation in the absence of mean flow (i.e., $M = 0$).

As shown in figure 2, attention is restricted to a duct of circular geometry with a cylindrical coordinate system (x, r, θ). For a duct with hard walls the boundary condition at $r = 1$ is that the acoustic particle velocity normal to the wall is zero.

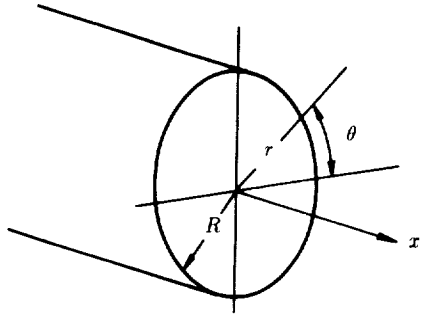

(a) Cylindrical coordinate system.

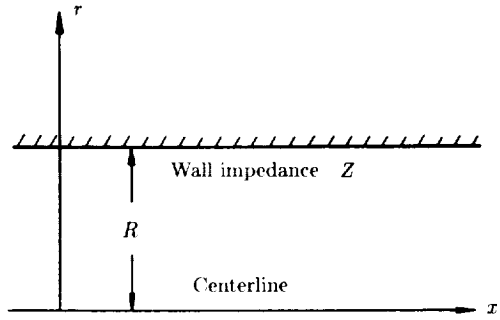

(b) Wall impedance configuration.

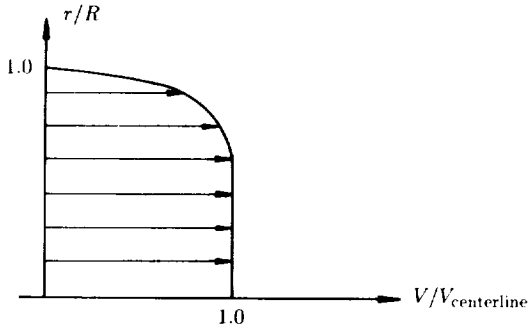

(c) Sheared velocity profile.

Figure 2. Geometrical, acoustical, and flow conditions for circular duct.

The coordinate r is scaled by the duct radius R. The acoustic momentum equation in the r direction shows that this is equivalent to the boundary condition at $r = 1$ as follows:

$$\frac{\partial p}{\partial r} = 0$$

At the duct centerline the boundary condition is that the solution should remain finite. It is assumed that an unspecified noise source introduces acoustic disturbances harmonically with time dependence $\exp(i\eta t)$, where $\eta = \omega R/c_r$, ω is the dimensional excitation frequency, and R is the duct radius. The resulting acoustic fluctuations in the duct can then be written

$$p(x, r, \theta, t) = P(x, r, \theta)\ \exp(i\eta t)$$

where $P(x, r, \theta)$ now satisfies a convected Helmholtz equation

$$(1 - M^2)\frac{\partial^2 P}{\partial x^2} + \nabla_c^2 P - 2i\eta M \frac{\partial P}{\partial x} + \eta^2 P = 0 \tag{14}$$

with boundary condition at $r = 1$ of

$$\frac{\partial P}{\partial r} = 0$$

and ∇_c is the gradient operator in the polar coordinate system (r, θ) (the coordinates in the duct cross section). Solutions to equation (14) can be written in terms of traveling waves as follows:

$$P_{mn}(x, r, \theta) = P(r)\ \exp(\pm im\theta)\ \exp(-ik_{x_{mn}} x)$$

where

$$\frac{k_{x_{mn}}}{\eta} = \frac{1}{1 - M^2}\left[-M \pm \sqrt{1 - (1 - M^2)\left(\frac{\kappa_{mn}}{\eta}\right)^2}\right] \tag{15}$$

The term $P(r)$ is then governed by the Bessel equation

$$\frac{d^2 P}{dr^2} + \frac{1}{r}\frac{dP}{dr} + \left(\kappa^2 - \frac{m^2}{r^2}\right) P = 0$$

with boundary condition at $r = 1$ of

$$\frac{dP}{dr} = 0$$

The solutions to this equation, finite at the origin, are $J_m(\kappa r)$, Bessel functions of the first kind of order m. The eigenvalues κ_{mn} are defined by

$$J'_m(\kappa_{mn}) = 0 \tag{16}$$

A solution to equation (14) and the hard-wall boundary condition is therefore

$$p_{mn}(x, r, \theta, t) = P_{mn} J_m(\kappa_{mn} r)\ \exp[i(\eta t \pm m\theta - k_{x_{mn}} x)] \tag{17}$$

There are an infinite number of such solutions, corresponding to integer values of m and to the infinite number of values κ_{mn} defined by the eigenvalue equation (16). These solutions are referred to as modes of propagation. At a fixed x, angular traveling waves (or spinning modes) of the form

$$p \propto \exp[i(\eta t \pm m\theta)]$$

are observed, while at fixed θ axial traveling waves of the form

$$p \propto \exp[i(\eta t - k_{x_{mn}} x)]$$

are observed. A given mode of propagation is thus the combination of a spinning mode and an axial traveling wave.

The parameter k_x is referred to as the axial wave number and can be real or complex depending on values of M, κ_{mn}, and η. For

$$(1 - M^2)\left(\frac{\kappa_{mn}}{\eta}\right)^2 < 1$$

k_x is real, and for most values of M, κ_{mn}, and η in this range k_x has a positive and a negative value corresponding to axial waves propagating in the positive and negative x-directions. If $M > 0$, over the range of parameters for which

$$1 < \left(\frac{\kappa_{mn}}{\eta}\right)^2 < \frac{1}{1 - M^2}$$

there are two negative values of k_x, but an acoustic energy argument (ref. 2) can be used to show that the positive sign in equation (15) still corresponds to acoustic power transmitted in the positive x-direction and the negative sign corresponds to acoustic power transmitted in the negative x-direction. A similar result showing two positive values for k_x applies if $M < 0$.

An interesting phenomenon occurs when

$$(1 - M^2)\left(\frac{\kappa_{mn}}{\eta}\right)^2 > 1$$

and k_x becomes complex:

$$\frac{k_{x_{mn}}}{\eta} = \frac{1}{1 - M^2}\left[-M \pm i\sqrt{(1 - M^2)\left(\frac{\kappa_{mn}}{\eta}\right)^2 - 1}\right]$$

In this case the solution of equation (17) becomes

$$p_{mn}(x, r, \theta, t) = P_{mn} J_m(\kappa_{mn} r)\ \exp\left\{i[\eta t \pm m\theta - \mathrm{Re}(k_x)x \pm \mathrm{Im}(k_x)x]\right\}$$

where

$$\mathrm{Re}(k_x) = -\frac{M\eta}{1 - M^2}$$

$$\mathrm{Im}(k_x) = \frac{\eta}{1 - M^2}\sqrt{(1 - M^2)\left(\frac{\kappa_{mn}}{\eta}\right)^2 - 1}$$

are the real and imaginary parts of the complex wave number $k_{x_{mn}}$. The traveling wave is attenuated with distance, the negative sign indicating the solution in the positive x-direction and the positive sign indicating the solution in the negative x-direction. An energy argument (ref. 2) shows that no acoustic power is associated with these modes.

Acoustic duct modes which are attenuated with distance and carry no acoustic power are referred to as being "cutoff," while modes which propagate in the usual sense are said to be "cut on." Reference 3 has introduced the terminology "cutoff ratio" for the parameter

$$\beta_{mn} = \frac{\eta}{\kappa_{mn}\sqrt{1 - M^2}}$$

When the cutoff ratio exceeds unity, the frequency is high enough that the mode corresponding to κ_{mn} is cut on. Values of cutoff ratio less than unity identify modes which are cutoff.

The exact physical phenomenon occurring in cutoff modes which produces attenuation with no source of dissipation is difficult to see in the presence of flow. However, reference 4 shows that in the case without mean flow the acoustic field of a piston driver in a duct is an entirely reactive field from which no acoustic power escapes when the cutoff ratio is less than unity.

In the classic work of Tyler and Sofrin (ref. 5), it is pointed out that if the noise source is such that only modes with cutoff ratios less than unity are produced, then in principle no acoustic power is propagated from the source. This could conceivably be accomplished with an isolated rotor, in which case a judicious choice of the number of blades and the rotational speed can ensure that the cutoff ratio is less than unity. However, the inevitable presence of struts and inlet or outlet guide vanes may produce interaction tones which propagate. In addition, the finite length of the inlet and outlet ducts allows the basically reactive field to radiate some power to the far field.

Another physical picture of the propagation, which is exact in a two-dimensional duct and is approximate in a circular duct, is that of viewing the acoustic field as the result of the interference of plane waves propagating at an angle to the duct axis and therefore reflecting from the duct walls. The angle of propagation is directly related to the cutoff ratio (ref. 6). When the cutoff ratio is unity, the angle of propagation is at 90° to the duct axis and the plane-wave propagation is just across the duct, a situation in which it would not be expected that acoustic power would be propagated down the duct.

Rice (ref. 3) also used an extended concept of modal cutoff ratio to good advantage in correlating attenuation in lined ducts and in estimating the direction of the major lobe of the radiation from a duct termination. This is discussed in a subsequent section.

The modal solutions of equation (17) are solutions which can exist within the duct. Whether they are actually present depends on the source and boundary conditions (so far not specified) where the duct terminates on the x-axis. In the case of an infinite duct (i.e., one extending $-\infty < x < \infty$), only waves traveling or decaying away from the source can be present. For a source at $x = 0$, only solutions with wave numbers appropriately defined for propagation or decay for $x > 0$ exist for $x > 0$, and those defined for propagation or decay for $x < 0$ exist for $x < 0$. This makes it necessary to choose the proper sign in equation (15). We can designate the wave numbers by $k^+_{x_{mn}}$ or $k^-_{x_{mn}}$ to indicate whether they apply to solutions traveling or decaying in the positive or the negative x-direction. Thus, for $x > 0$ an appropriate solution is

$$p_{mn}(x, r, \theta, t) = P^+_{mn} J_m(\kappa_{mn} r) \exp[i(\eta t \pm m\theta - k^+_{x_{mn}} x)]$$

and for $x < 0$ an appropriate solution is

$$p_{mn}(x, r, \theta, t) = P^-_{mn} J_m(\kappa_{mn} r) \exp[i(\eta t \pm m\theta - k^-_{x_{mn}} x)]$$

In the case of a duct of finite length, boundary conditions must be specified at the terminations or the duct model must be coupled to some other description of the acoustic propagation beyond the termination. In any case, the terminations introduce reflections, and solutions corresponding to both k_x^+ and k_x^- can be present at any point in the duct.

In most cases it is not possible to write a boundary condition at a duct termination. For example, in the case of a duct terminating at free space, the acoustic response of the medium outside the duct establishes the boundary condition. Therefore the duct and radiation problems must be solved simultaneously. This matter is discussed more in a subsequent section.

Because of the difficulty with precise definition of termination conditions, two approximate ones are often introduced. At low frequencies the assumption of zero acoustic pressure for a termination at free space is reasonable. This "pressure release" boundary condition produces complete reflection of traveling waves and does not permit any acoustic power to escape from the duct. It is only useful for the study of standing waves (the interaction of waves traveling in both directions) in ducts where only the plane wave propagates.

The much more common assumption is that the termination is reflection free or that the duct is of infinite length. This assumption is difficult to justify for unlined ducts in which traveling waves are not attenuated; however, for relatively high frequencies (wavelength small relative to the duct radius) and for frequencies other than those approaching cutoff frequencies, reflections from open ends are small. For lined ducts, as shown subsequently, reflections may be even less important because the incident amplitudes are considerably reduced before reaching the termination.

General solutions to the convected wave equation for the circular duct can be given as a superposition of the eigenfunction solutions (eq. (17)) to yield

$$p(x,r,\theta,t) = \sum_{m=-\infty}^{\infty} \sum_{n=0}^{\infty} P_{mn} J_m(\kappa_{mn} r)\ \exp\left[i(\eta t - m\theta - k_{x_{mn}}^{\pm} x)\right]$$

$$p(x,r,\theta,t) = \sum_{m=-\infty}^{\infty} \sum_{n=0}^{\infty} J_m(\kappa_{mn} r)\ \exp\left[i(\eta t - m\theta)\right]$$

$$\times \left[P_{mn}^{+}\ \exp(-ik_{x_{mn}}^{+} x) + P_{mn}^{-}\ \exp(-ik_{x_{mn}}^{-} x)\right]$$

The values of the amplitude coefficients depend on the nature of the source. For example, if we were interested in acoustic propagation in the positive x-direction in an infinite duct, for which there is no reflection at the termination and therefore no waves propagating in the negative x-direction, the series would be

$$p(x,r,\theta,t) = \sum_{m=-\infty}^{\infty} \sum_{n=0}^{\infty} P_{\mu n} J_\mu(\kappa_{\mu n} r)\ \exp\left[imN(\Omega t - \theta)\right]\ \exp(-ik_{x_{\mu n}}^{+} x)$$

for a noise source consisting of a simple rotor with N blades turning at angular speed Ω. For this equation, $\mu = mN$, the $k_{x_{\mu n}}^{+}$ are limited to the proper choices for solutions with $x > 0$, and the modal amplitudes P_{mn} depend on the blade loading.

In this case the solution is spinning modes at frequency $mN\Omega$, locked in phase with the rotor. For interaction of rotor and stator or of rotor and inlet guide vanes, all modes are not spinning in the same direction and with the same angular speed as the rotor. Reference 5 gives an excellent description of the influence of the noise source on the modal character of the acoustic propagation in the duct.

Attenuation Calculations in Lined Uniform Ducts

In the previous section fundamental properties of sound propagation in uniform hard-wall ducts with uniform flow were introduced. In this section we deal with the more practically important problem of the calculation of the axial wave number, and hence the attenuation, in uniform ducts with acoustically treated walls. The ducts considered in general contain a mean flow which in the least restrictive case can have a sheared velocity profile approximating the gross effects of the viscous boundary layer.

Attenuation calculations for acoustic transmission are required in aircraft turbofan engine inlet and exhaust ducts. Problems of this type are demanding not only because of the acoustic environment involved, but also because of requirements for computational efficiency and accuracy for design studies.

The duct geometry specifically considered in this discussion is circular. Where appropriate, results are also quoted without proof for two-dimensional rectangular geometries. Most of the results can be directly extended to annular and three-dimensional rectangular ducts. Figure 2 shows the pertinent geometrical details for the circular duct.

The Physical Problem

The uniform duct carries a mean flow which is uniform axially but nonuniform radially. The mean density and pressure are assumed to be uniform. The sound transmission problem is one of modeling acoustic fluctuations on this mean flow. This representation is consistent with the developments of reference 7, which starts from the full viscous equations of compressible fluid mechanics and, with a series of approximations and assumptions, arrives at this model, which captures the important features of the refractive effects of sheared viscous flow on sound propagation.

The field equations which are appropriate are equations (5), (6), and (8), restricted to the case when ρ_o, p_o, and c_o are constant ($\rho_o = 1$, $p_o = 1$, and $c_o = 1$) and $\mathbf{V}_o = M(r)\mathbf{e}_x$:

$$\frac{\partial p}{\partial t} + M\frac{\partial p}{\partial x} + \nabla \cdot \mathbf{V} = 0 \tag{18}$$

$$\frac{\partial \mathbf{V}}{\partial t} + M\frac{\partial \mathbf{V}}{\partial x} + \nabla p + \frac{dM}{dr}v_r\mathbf{e}_x = 0 \tag{19}$$

where

$$\mathbf{V} = v_x\mathbf{e}_x + v_r\mathbf{e}_r + v_\theta\mathbf{e}_\theta$$

Equations (18) and (19) can be combined as

$$\left(\frac{\partial}{\partial t} + M\frac{\partial}{\partial x}\right)^3 p = \left(\frac{\partial}{\partial t} + M\frac{\partial}{\partial x}\right)\nabla^2 p - 2\frac{dM}{dr}\frac{\partial^2 p}{\partial x\,\partial r} \tag{20}$$

Note that if $M(r)$ is constant, $dM/dr = 0$ and equation (20) becomes

$$\left(\frac{\partial}{\partial t} + M\frac{\partial}{\partial x}\right)\left[\left(\frac{\partial}{\partial t} + M\frac{\partial}{\partial x}\right)^2 - \nabla^2\right] p = 0 \tag{21}$$

For harmonic excitation proportional to $\exp(i\eta t)$, with $\eta = \omega R/c_r = 2\pi f R/c_r$ (where $\omega = 2\pi f$ is the driving frequency), we seek solutions in the form

$$p(x, r, \theta, t) = \hat{p}(x, r, \theta)\ \exp(i\eta t)$$

The resulting equation for $p(x, r, \theta)$ is

$$\left(i\eta + M\frac{\partial}{\partial x}\right)^3 \hat{p} = \left(i\eta + M\frac{\partial}{\partial x}\right)\nabla^2\hat{p} - 2\frac{dM}{dr}\frac{\partial^2\hat{p}}{\partial x\,\partial r}$$

Traveling wave solutions in the form

$$\hat{p}(x, r, \theta) = P(r)\ \exp(\pm im\theta - ik_x x)$$

are sought. The term $P(r)$ satisfies the ordinary differential equation

$$\frac{d^2P}{dr^2} + \left[\frac{1}{r} + \frac{2(k_x/\eta)}{(1 - Mk_x/\eta)}\frac{dM}{dr}\right]\frac{dP}{dr} + \left\{\eta^2\left[\left(1 - M\frac{k_x}{\eta}\right)^2 - \left(\frac{k_x}{\eta}\right)^2\right] - \frac{m^2}{r^2}\right\} P = 0 \tag{22}$$

The boundary condition at the duct wall ($r = 1$) is based on the assumption that the lining is locally reacting and that the relationship between nondimensional pressure and nondimensional lining particle velocity v_ν is

$$\frac{p}{v_\nu} = \frac{Z}{\rho_r c_r} \tag{23}$$

where $Z/\rho_r c_r$ is the wall nondimensional specific impedance. At the duct wall the fluid particle displacement and the wall particle displacement are the same. Note that because of the convection effect of the mean flow, the fluid particle velocity is the convective, or substantial, derivative of the fluid particle displacement. When the Mach number at the wall vanishes so does this convection effect. Thus, if ζ is the particle displacement of the wall directed into the wall in the inward normal direction $\boldsymbol{\nu}$, then

$$\mathbf{V}\cdot\boldsymbol{\nu} = \left(i\eta + M\frac{\partial}{\partial x}\right)\zeta \tag{24}$$

where $\mathbf{V}\cdot\boldsymbol{\nu}$ is the fluid particle velocity in the normal direction of the wall and directed into the wall. Since the nondimensional wall particle velocity v_ν is related to the particle displacement by

$$v_\nu = i\eta\varsigma$$

equation (24) becomes

$$\mathbf{V} \cdot \boldsymbol{\nu} = \left(1 - i\frac{M}{\eta}\frac{\partial}{\partial x}\right) v_\nu \tag{25}$$

We can now replace v_ν by using equation (23) to obtain

$$\mathbf{V} \cdot \boldsymbol{\nu} = A\left(1 - i\frac{M}{\eta}\frac{\partial}{\partial x}\right) p$$

where $A = \rho_r c_r / Z$ is the wall nondimensional specific acoustic admittance.

In the case of the circular duct, $v_\nu = v_r$. The radial component of the acoustic momentum equation (19) is

$$\left(\frac{\partial}{\partial t} + M\frac{\partial}{\partial x}\right) v_r = -\frac{\partial p}{\partial r}$$

This is used to rewrite the boundary condition (eq. (25)) entirely in terms of the acoustic pressure:

$$\frac{\partial p}{\partial r} = -i\eta A\left(1 - i\frac{M}{\eta}\frac{\partial}{\partial x}\right)^2 p \tag{26}$$

Equation (26) is to be enforced on solutions of equation (22) at $r = 1$. The boundary condition at $r = 0$ is that the solution should remain finite. The field equation (22), the boundary condition equation (26), and the finiteness condition at $r = 0$ constitute an eigenvalue problem of finding values of the wave number k_x such that the homogeneous differential equation and homogeneous boundary conditions have a nontrivial solution. We now consider special cases of importance.

The Eigenvalue Problem

Sheared Flow With No-Slip Boundary Conditions

It is assumed that the sheared velocity profile is known, so that we are given $M(r)$ and dM/dr and specify $M = 0$ at the duct wall. In the circular-duct case we have shown that the field equations can be combined to yield

$$\frac{d^2P}{dr^2} + \left[\frac{1}{r} + \frac{2(k_x/\eta)}{1 - (Mk_x/\eta)}\frac{dM}{dr}\right]\frac{dP}{dr} + \left\{\eta^2\left[\left(1 - M\frac{k_x}{\eta}\right)^2 - \left(\frac{k_x}{\eta}\right)^2\right] - \frac{m^2}{r^2}\right\}P = 0$$

which is equation (22). The boundary conditions at $r = 0$ and $r = 1$ are

$$\left.\begin{aligned} P(0) &= \text{Finite} \\ \frac{dP}{dr}(1) &= -i\eta AP \end{aligned}\right\} \tag{27}$$

Since many of the results in the literature are quoted for two-dimensional ducts, it is appropriate to state here the eigenvalue problem for this case with a lined wall at $y = 1$ and a hard wall at $y = 0$ as

$$\frac{d^2P}{dy^2} + \frac{2(k_x/\eta)}{1-(Mk_x/\eta)}\frac{dM}{dy}\frac{dP}{dy} + \eta^2\left[\left(1 - M\frac{k_x}{\eta}\right)^2 - \left(\frac{k_x}{\eta}\right)^2\right]P = 0 \tag{28}$$

with boundary conditions at $y = 0$ and $y = 1$ of

$$\left.\begin{aligned}\frac{dP}{dy}(0) &= 0\\ \frac{dP}{dy}(1) &= -i\eta AP\end{aligned}\right\} \tag{29}$$

where $\eta = \omega b/c_r = 2\pi f b/c_r$, where b is the duct height.

A two-dimensional duct with two symmetrically lined walls at $y = 1$ and $y = -1$ can be treated by also solving the boundary value problem with $P = 0$ at $y = 0$. The eigenfunction solutions from the boundary conditions in equations (29) are then the symmetric solutions and those generated with $P = 0$ at $y = 0$ are the antisymmetric solutions.

Uniform Mean Flow

In this case it is assumed that the mean flow Mach number is uniform across the duct. Therefore, $dM/dr = 0$. An interesting preliminary result can be obtained from equations (18), (19), and (21). In addition to equation (21), equations (18) and (19) can be combined to yield

$$\left(\frac{\partial}{\partial t} + M\frac{\partial}{\partial x}\right)\left[\left(\frac{\partial}{\partial t} + M\frac{\partial}{\partial x}\right)^2 - \nabla^2 - \nabla\times\nabla\times\right]\mathbf{V} = 0 \tag{30}$$

Equation (19) is used to show that

$$\left(\frac{\partial}{\partial t} + M\frac{\partial}{\partial x}\right)(\nabla\times\mathbf{V}) = 0 \tag{31}$$

This implies that vorticity is convected or it vanishes. In combination with equation (30) this means that the velocity field satisfies

$$\left(\frac{\partial}{\partial t} + M\frac{\partial}{\partial x}\right)^3\mathbf{V} - \nabla^2\left(\frac{\partial}{\partial t} + M\frac{\partial}{\partial t}\right)\mathbf{V} = 0 \tag{32}$$

From equation (30) or (32) it is shown that there are solutions for which

$$\left(\frac{\partial}{\partial t} + M\frac{\partial}{\partial x}\right)\mathbf{V} = 0$$

From equation (19), these solutions have $\nabla p = 0$, which implies that the perturbation pressure field vanishes, and therefore

$$\nabla \cdot \mathbf{V} = 0$$

Hence, there exists a class of velocity solutions satisfying the incompressible continuity equation, with vanishing pressure perturbations which are convected with the mean flow. For harmonic traveling waves of the form

$$\mathbf{V}(x, r, \theta, t) = \mathbf{V}(r)\ \exp(\pm im\theta)\ \exp[i(\eta t - k_x x)]$$

this means

$$(i\eta - iMk_x)\mathbf{V} = 0$$

or

$$k_x = \frac{\eta}{M} = \frac{\omega R}{V} \tag{33}$$

The traveling waves are thus of the dimensional form

$$\mathbf{V}(x, r, \theta, t) = \mathbf{V}(r)\ \exp(\pm im\theta)\ \exp\left\{i\omega[t - (x/V)]\right\}$$

This is a disturbance for which in general $\nabla \times \mathbf{V} \neq 0$ and which is propagating at the mean flow velocity. This solution with vorticity is convected with the flow. This is termed a hydrodynamic disturbance.

A second type of solution has $\nabla \times \mathbf{V} = 0$ (eq. (31)) and is therefore irrotational. These solutions satisfy

$$\left(\frac{\partial}{\partial t} + M\frac{\partial}{\partial x}\right)^2 p - \nabla^2 p = 0$$

and are the acoustic fluctuations. It is thus observed that in uniform flow hydrodynamic (rotational) disturbances and acoustic (irrotational) fluctuations can be separated.

The above observations are not generally true when the flow is sheared, and in that case acoustic disturbances are not irrotational (ref. 8). However, there are still hydrodynamic disturbances in the sheared flow. Reference 8 discusses this in the case of a linear shear profile. The main point to be made here is that the hydrodynamic solutions are contained in the field equations, even with $dM/dr = 0$, although the solutions are not generally retained in the development of the convected wave equation.

We now write the eigenvalue problem for the acoustic disturbances in the case of uniform flow. In the circular-duct case,

$$\frac{1}{r}\frac{d}{dr}\left(r\frac{dP}{dr}\right) + \left\{\eta^2\left[\left(1 - M\frac{k_x}{\eta}\right)^2 - \left(\frac{k_x}{\eta}\right)^2\right] - \frac{m^2}{r^2}\right\}P = 0 \tag{34}$$

with boundary conditions at $r = 0$ and $r = 1$ of

$$\left.\begin{aligned} P(0) &= \text{Finite} \\ \frac{dP}{dr}(1) &= -i\eta A\left(1 - M\frac{k_x}{\eta}\right)^2 P \end{aligned}\right\} \tag{35}$$

and in the two-dimensional case,

$$\frac{d^2P}{dy^2} + \eta^2 \left[\left(1 - M\frac{k_x}{k} \right)^2 - \left(\frac{k_x}{\eta} \right)^2 \right] P = 0 \tag{36}$$

with boundary conditions at $y = 0$ and $y = 1$ of

$$\left.\begin{aligned} \frac{dP}{dy}(0) &= 0 \\ \frac{dP}{dy}(1) &= -i\eta A \left(1 - M\frac{k_x}{\eta} \right)^2 P \end{aligned}\right\} \tag{37}$$

As noted previously, the boundary conditions (eqs. (37)) generate symmetric solutions for the duct spanning $-1 \leq y \leq 1$. Antisymmetric solutions arise from $P = 0$ at $y = 0$.

No Mean Flow

For no mean flow, $M = 0$. In the circular-duct case, the eigenvalue problem is given by

$$\frac{1}{r}\frac{d}{dr}\left(r\frac{dP}{dr} \right) + \left\{ \eta^2 \left[1 - \left(\frac{k_x}{\eta} \right)^2 \right] - \frac{m^2}{r^2} \right\} P = 0 \tag{38}$$

with boundary conditions at $r = 0$ and $r = 1$ of

$$\left.\begin{aligned} P(0) &= \text{Finite} \\ \frac{dP}{dr}(1) &= -i\eta AP \end{aligned}\right\} \tag{39}$$

In the two-dimensional duct,

$$\frac{d^2P}{dy^2} + \eta^2 \left[1 - \left(\frac{k_x}{\eta} \right)^2 \right] P = 0 \tag{40}$$

with boundary conditions at $y = 0$ and $y = 1$ of

$$\left.\begin{aligned} \frac{dP}{dy}(0) &= 0 \\ \frac{dP}{dy}(1) &= -i\eta AP \end{aligned}\right\} \tag{41}$$

Antisymmetric eigenfunction solutions follow from $P = 0$ at $y = 0$, as noted previously.

The boundary value problems described by equations (28) and (29) and (34) to (41) are eigenvalue problems in which we seek nontrivial solutions to the differential equation which satisfy the specified boundary conditions. The eigenvalue in each case is the axial wave number k_x/η which contains the essential attenuation information.

In each case the boundary value problem defines an infinite sequence of eigenvalues. Corresponding to each eigenvalue is a nontrivial solution, or eigenfunction, which defines a transverse pressure variation $P_{mn}(r)$ or $P_n(y)$ which propagates according to

$$p_{mn}(x, r, \theta, t) = P_{mn}(r) \ \exp[i(\eta t \pm m\theta - k_{x_{mn}} x)] \tag{42}$$

or

$$p_n(x, y, t) = P_n(y) \ \exp[i(\eta t - k_{x_n} x)] \tag{43}$$

The amplitudes of the eigenfunction are suitably normalized. Each such solution defines a mode of propagation. In general, the acoustic field in a duct is a superposition of these nodes with amplitudes dependent on the source and termination conditions

$$p(x, r, \theta, t) = \sum_{m=-\infty}^{\infty} \sum_{n=0}^{\infty} A_{mn} P_{mn}(r) \ \exp[i(\eta t \pm m\theta - k_{x_{mn}} x)] \tag{44}$$

or

$$p(x, y, t) = \sum_{n=1}^{\infty} A_n P_n(y) \ \exp[i(\eta t - k_{x_n} x)] \tag{45}$$

As previously discussed, some of the solutions correspond to propagation in the positive x-direction, while the remainder correspond to propagation in the negative x-direction.

The eigenvalue problems so described are not true Sturm-Liouville problems so that there is no general statement about orthogonality of the eigenfunctions. However, in the no-flow case it can be shown that

$$\int_0^1 r P_{mn}(r) P_{mk}(r) \, dr = M_{nn} \, \delta_{nk}$$

or

$$\int_0^1 P_n(y) P_k(r) \, dr = M_{nn} \, \delta_{nk}$$

where $\delta_{nk} = 0$ for $n \neq k, \delta_{nk} = 1$ for $n = k$, and

$$M_{nn} = \int_0^1 r P_{mn}^2 \, dr$$

or

$$M_{nn} = \int_0^1 P_n^2(y) \, dy$$

This orthogonality is not found in general when mean flow is present. The eigenfunctions are orthogonal for any uniform mean flow when the walls are hard ($A = 0$).

Calculation of Attenuation

In all the eigenvalue problems postulated we have sought solutions in the form

$$p(\mathbf{r}, x, t) = P(\mathbf{r}) \ \exp[i(\eta t - k_x x)] \tag{46}$$

Here, the harmonic time dependence is explicitly included. The term $\mathbf{r}$ is the vector of coordinates transverse to the duct axis. Attenuation is defined as the change in sound pressure level (SPL) over a specified length of duct. In the present case only ducts without end reflections are considered, so that attenuation is based only on transmitted modes. Furthermore, the attenuation is considered in each mode separately. The extension to multimode propagation is straightforward but yields a considerably complicated result. SPL is defined as

$$\text{SPL} = 20 \ \log \frac{\overline{P}}{P_o}$$

where $\overline{P}$ is the root-mean-squared acoustic pressure and P_o is a suitable reference (by convention for aeroacoustics, this is taken as $P_o = 20 \ \mu Pa$). The change in SPL over length Δx is

$$\Delta \ \text{SPL} = 20 \ \log \frac{\overline{P}_2}{\overline{P}_1} = 20 \ \log \frac{\overline{P}(x + \Delta x)}{\overline{P}(x)}$$

If $k_x = \alpha + i\beta$, it follows that

$$\frac{\overline{P}_2(x + \Delta x)}{\overline{P}_1(x)} = \exp(\beta \ \Delta x)$$

Thus,

$$\Delta \ \text{SPL} = (20 \ \log e)\beta \ \Delta x = 8.686\beta \ \Delta x \tag{47}$$

For a decaying wave, β is negative if the propagation is in the positive x-direction.

Thus, calculation of attenuation requires the solution of the eigenvalue problem for k_x.

Solution of the Eigenvalue Problem

In this section we discuss techniques for the solution of the eigenvalue problems posed in the previous section. Emphasis is on numerical techniques, although it is appropriate to refer to some methods which were developed prior to the availability of computer systems.

No Mean Flow

When the mean flow vanishes, the eigenvalue equation for the circular duct is equation (38) and the associated boundary conditions. This can be written in slightly modified form to yield

$$\frac{d^2P}{dr^2} + \frac{1}{r}\frac{dP}{dr} + \left(\kappa^2 - \frac{m^2}{r^2}\right) P = 0 \tag{48}$$

with boundary conditions (eqs. (39)) at $r = 0$ and $r = 1$ of

$$P(0) = \text{Finite}$$

$$\frac{dP}{dr}(1) = -i\eta AP$$

where

$$\kappa^2 = \eta^2 \left[1 - \left(\frac{k_x}{\eta}\right)^2\right] \tag{49}$$

Solutions to equation (48), satisfying the boundary condition at $r = 0$, are Bessel functions of the first kind of order m:

$$P = J_m(\kappa r)$$

The eigenvalue κ is determined from the boundary condition at the outer wall ($r = 1$) according to

$$\kappa \frac{J'_m(\kappa)}{J_m(\kappa)} = -i\eta A \tag{50}$$

There are an infinite number of discrete eigenvalues κ of equation (50). If these are enumerated by the angular mode number m and the radial mode number n, then from equation (49) the modal wave numbers are given by

$$\left(\frac{k_x}{\eta}\right)_{mn} = \pm\sqrt{1 - \left(\frac{\kappa_{mn}}{\eta}\right)^2} \tag{51}$$

The equivalent two-dimensional problem which follows from equation (40) leads to the eigenvalue problem

$$\kappa \tan \kappa = i\eta A \tag{52}$$

and the corresponding sequences of eigenfunction solutions

$$P_n = \cos \kappa_n y$$

These are also the symmetric solutions for $-1 \leq y \leq 1$, as previously noted. The antisymmetric solutions follow from the eigenvalue equation $\kappa \cot \kappa = -i\eta A$ and the eigenfunction solutions are $\sin \kappa_n y$. Equation (51) for the axial wave number still holds in the two-dimensional case.

The determination of the eigenvalues of equation (50) or (52) is a conceptually simple proposition. In practice it is not simple because of the topography of the complex functions of the complex variable κ the zeros of which are the eigenvalues and because of the complex arithmetic which must be performed. Because of these difficulties, early researchers were led to consider approximations. Sivian (ref. 9) and Molloy (ref. 10) arrived at essentially the same end result by different means. They used a one-dimensional propagation assumption. Sivian cast the problem as an electrical analog and Molloy used the acoustical equations directly, making his

results generally more accessible to the present generation of acousticians. Molloy also provided charts from which attenuation can be obtained directly. No restriction was placed on the shape of the duct cross section and the lining could have been circumferentially varying, provided the assumption of plane-wave propagation was adhered to. This is a low-frequency approximation consistent with the restriction to nearly plane waves and one would expect it to require relatively small wall admittance to maintain the planar approximation. This approach has the advantage of producing a direct calculation formula for the attenuation.

Perhaps one of the best known estimates of duct attenuation is presented by Sabine (ref. 11). He used the Sivian-Molloy results and his own experiments on rectangular ducts with relatively weak attenuation to establish the attenuation estimate

$$\frac{\Delta \text{ SPL}}{\Delta x} = 12.6\alpha^{-0.25} P_e/S \tag{53}$$

where Δx is the duct length in feet, α is the reverberation chamber absorption coefficient for the duct lining, P_e is the lined perimeter in inches, and S is the cross-sectional area in square inches.

The first direct attack on equation (52) for rectangular ducts appears to be presented in Morse's well-known work in references 12 and 13. Rather than attempt to solve equation (52) explicitly, Morse treated it as a conformal transformation from the κ plane to the admittance plane. He effectively picked values of κ and computed values of A. Level curves of the complex admittance were then drawn on the plane whose axes were the real and imaginary parts of κ. Morse and Ingard (ref. 13) also presented charts from which κ and hence k_x/η can be determined. They used an entirely different notation and presented the plots in a format so that the charts can be used for one or two lined walls. Great care must be exercised to fully understand the proper chart interpretation. Cremer (ref. 14) also gave a thorough discussion of the chart procedure in the rectangular-duct case. He discussed the importance of branch points of the conformal transformation in determining an optimum attenuation based on the coalescing of two modes of propagation.

In the circular-duct case, equation (50) can be rewritten through use of a recurrence relation for the Bessel function derivative to yield

$$\kappa \frac{J_{m-1}(\kappa)}{J_m(\kappa)} - m = -i\eta A \tag{54}$$

Note that if $m = 0$, $J_{-1}(\kappa) = -J_1(\kappa)$. Morse and Ingard (ref. 13) also presented charts for this case. Reference 13 presents a Morse Chart with $m = 0$ and $m = 1$, again with a different notation. Molloy and Honigman (ref. 15) also addressed the circular-duct problem and apparently first produced what is effectively a Morse Chart for the $m = 0$ case.

A feature of the Morse Charts which makes them particularly useful in applications is that only a single chart is needed for all duct configurations. Only ηA is required. This embodies the complete specification of the frequency, duct size, and lining admittance. This feature is lost when mean flow is present, as shown subsequently.

What appears to be the first attempt to produce a direct solution of equation (52) in the rectangular-duct case is presented in reference 16. The approach was to expand

the eigenvalue equation in a power series in κ and then use a standard technique to invert the power series to obtain a power series defining η.

A contribution of substantial importance for future investigators was made in reference 17. Addressed therein was the problem of axially symmetric propagation in a circular duct, for which equation (54) becomes

$$\kappa \frac{J_1(\kappa)}{J_0(\kappa)} = i\eta A \tag{55}$$

If the definitions

$$y = \frac{i\eta A}{2}$$

$$w = \left(\frac{\kappa}{2}\right)^2$$

are introduced and if equation (55) is differentiated with respect to y, through use of recurrence relations for Bessel function derivatives, the following differential equation for w results:

$$(w + y^2)\frac{dw}{dy} = w \tag{56}$$

Reference 17 sought the lowest mode eigenvalue for $m = 0$ and thus sought the solution of equation (55), which at $y = 0$ has $w = 0$. It used a power series expansion, and under the assumption that y is small, it found the solution is approximated by

$$w = 1 - \exp(-y)$$

For present applications the reference 17 result is of limited value, but Rice (ref. 18) has extended it to higher order symmetric modes by considering series solutions having initial conditions at $y = 0$, which are the hard-wall eigenvalues for any desired number of modes. He also set the problem up specifically for large admittances and used initial values corresponding to the perfectly soft-wall eigenvalues. Convergence is a problem in either case near the branch cut delineating the modal regions, and a common nonlinear equation solving routine is used when this is encountered.

Benzakein, Kraft, and Smith (ref. 19) and Zorumski and Mason (ref. 20) have extended the method to nonsymmetric eigenvalues and have used numerical integration. The differential equation derived by differentiation of equation (50) or equation (54) and the use of recurrence relations for the Bessel function derivatives is

$$\frac{d(\kappa/\eta)}{dA} = \frac{i\kappa}{(\kappa^2 - m^2) - (\eta A)^2} \tag{57}$$

This equation is integrated numerically with starting conditions corresponding to $\mathrm{Re}(A) = 0$. When $\mathrm{Re}(A) = 0$, equation (50) has only real eigenvalues which are easily found with a real search routine to yield the starting values for κ. The differential equation is then integrated along a path with $\mathrm{Im}(A) = \text{Constant}$. If $A = \mathrm{Re}(A) + i\mathrm{Im}(A)$ is the actual admittance, then the integration is along the path

$A = x + i\mathrm{Im}(A)$ $(0 \leq x \leq \mathrm{Re}(A))$, and the value of κ when $x = \mathrm{Re}(A)$ is the desired eigenvalue. Reference 20 shows some example calculations, but little is stated about the performance of the method.

Doak and Vaidya (ref. 21) have considered the nature of the eigenvalues of equation (50) in the circular-duct case and have looked at approximations of particular interest in the limit of small ηA and large A.

Perhaps the most obvious eigenvalue solution technique, the simple Newton-Raphson iteration, is notoriously unreliable as a general-purpose method for calculations involving many modes. This is because of the topography of the function for which zeros are sought. In certain instances very accurate starting values are required if convergence to a nearby root is to be achieved, and all users will attest to numerous instances when the same root is found with two different starting values or when unwanted roots are found. Christie (ref. 22) has published his approach to the use of the Newton-Raphson iteration to find the lowest order mode for a rectangular duct. He starts at low frequency. The lowest eigenvalue has $|\kappa| << 1$, where equation (52) can be written for $|\kappa| << 1$ (the lowest mode eigenvalue) as

$$\kappa^2 = i\eta A$$

The frequency is incremented and this result is used as the next starting value. This proceeds until the desired frequency is reached. This type of incrementing process minimizes the chance of unpredictable convergence. For higher order modes starting values ascending in integer multiples of π could be used. The Newton-Raphson iteration is particularly useful for refining eigenvalue estimates arrived at by other methods, such as the integration scheme of reference 20.

Other methods which have appeared in the literature to deal with the eigenvalue problem come under the general category of discretization techniques. In these methods the differential equation which governs the transverse variation of pressure in the duct (e.g., eq. (38) or (40)) is replaced by a set of algebraic equations based on a finite-difference method (FDM), a finite-element method (FEM), or a method of weighted residuals (MWR). These methods are probably too costly for circular geometries with uniform linings and rectangular geometries with uniform linings on each wall. However, they may be the only approach when the lining varies peripherally in an arbitrary way or when the duct cross section is not circular, rectangular, or some other geometry for which the Helmholtz equation has separable solutions. These methods are considered in more detail in subsequent sections. However, explicit examples of their use in the no-flow case can be found in references 23 and 24.

Uniform Mean Flow

When uniform mean flow is present, the eigenvalue problem becomes somewhat more complicated. The reduction to a transcendental eigenvalue equation follows exactly the procedure previously described. The analytic representation of the transverse pressure variation remains unchanged, but the eigenvalue equations become more complex. In the circular-duct case,

$$\kappa \frac{J'_m(\kappa)}{J_m(\kappa)} = -i\eta A \left(1 - M\,\frac{k_x}{\eta}\right)^2 \tag{58}$$

with

$$\frac{k_x}{\eta} = \frac{1}{1-M^2}\left[-M \pm \sqrt{1-(1-M^2)\left(\frac{\kappa}{\eta}\right)^2}\right]$$

In the two-dimensional-duct case,

$$\kappa \tan \kappa = i\eta A\left(1 - M\frac{k_x}{\eta}\right)^2 \tag{59}$$

with k_x/η as defined in the circular-duct case. Both of these eigenvalue problems can be viewed as a single, very complicated transcendental equation (if k_x/η is inserted into eq. (58) or (59) from the auxiliary equation) or as a coupled pair of equations.

The Morse method (refs. 12 and 13) becomes very unattractive for general calculations because the chart must be a conformal transformation from the κ plane to the ηA plane, with Mach number as a parameter. Thus, a separate chart for each Mach number is required. This approach has been used, but direct eigenvalue solutions are certainly of more general interest.

Reference 25 presents an interesting approximate solution technique in its study of bulk liners with an infinite backing space. This case yields a purely resistive lining, and with certain restrictions it arrived at the eigenvalue equation

$$\kappa \tan \kappa = i\eta A\left(1 - M\frac{k_x}{\eta}\right)$$

with k_x/η as previously defined in connection with equations (58) and (59). Note that the quantity $1 - M(k_x/\eta)$ appears to the first power and corresponds to a boundary condition based on continuity of particle velocity. (See the discussion of eqs. (23) and (24) regarding particle velocity and particle displacement.) This approach involved introducing an approximation for the tangent function and then obtaining a direct algebraic solution of the resulting equation.

An early direct eigenvalue solution was presented in reference 26. The method, applied to a two-dimensional duct, considered first the no-flow case. The no-flow eigenvalues were quickly estimated from a Morse Chart and used as initial estimates for a simple Newton-Raphson iteration. Eigenvalues thus determined are initial estimates for a case with a slightly incremented Mach number. Equation (59) is then solved by a combination of relaxation and Newton-Raphson iteration, the right-hand side being constructed from a previous estimate of k_x/η to form an effective admittance. At each stage of relaxation the Newton-Raphson iteration is used to calculate a new κ and k_x/η. Relaxation is carried out until convergence occurs. The Mach number is then incremented and the procedure repeated until the final Mach number is reached. The method was used for a number of calculations with little difficulty, but it has the disadvantage of requiring a solution for the no-flow problem. It is thus not a stand-alone method.

The approximation scheme developed in reference 21 for the circular duct in the no-flow case was extended to the case when flow is present. This extension first solved the problem for κ in the zero admittance case, and under the assumption of small ηA it used this solution in equation (58) to evaluate the right-hand side. This yielded a no-flow problem with an effective admittance to which the previously derived

approximation scheme for small ηA was applied. If the solutions were iterated to make successive approximations converge, the principle would have been essentially that in reference 26.

Ko (ref. 27) has made extensive calculations for the eigenvalues in a rectangular duct with two opposing walls lined. For symmetric modes the two-dimensional eigenvalue equation (59) applies, and for antisymmetric modes a second eigenvalue equation involving the cotangent applies. Ko's method of solution involves beginning with the nearly hard-wall case ($A = 0$) and using the eigenvalues so determined as initial estimates for a Newton-Raphson iteration. The driving frequency is incremented from zero to the required value, but Ko did not fully specify the manner in which the starting values are assigned with each new frequency increment. In reference 28, Ko reported the same type of method and results for a circular duct. He did not comment on the reliability of the Newton-Raphson approach, and this could be substantially affected by the incrementing and initial guess procedures.

A refinement of the Newton-Raphson iteration scheme has been used in reference 29. Instead of a Newton-Raphson iteration, a second-order method known as Bailey's method (ref. 30) was used, which is different in that it requires a second derivative but is used in exactly the same way as a Newton-Raphson iteration. In addition, a detailed study of the topography of the Morse Charts for both zero and uniform mean flow was made. In the case of mean flow, the Morse Charts are severely distorted with increasing Mach number and expand across the $\mathrm{Re}(\kappa)$ axis (at $M = 0$ all permissible solutions lie in one quadrant in the upper half-plane of κ). The starting point in the analysis is the $M = 0$ case. Based on considerable investigation, the Morse Chart (which is universal for any ηA when $M = 0$) is divided into subregions. Depending on the given value of ηA, the starting value for the Bailey iteration is chosen in a subregion near the ηA value. Convergence to the proper eigenvalue is then relatively certain. Mach number is then incremented with the previous Mach number results used for the starting values. It is reported that the result of this development is a reliable computational scheme. A modal identification scheme based on the Morse Charts has been used in reference 29 and further expanded upon in reference 31.

A worker entering the field and needing to develop a stand-alone computational scheme would probably wish to circumvent the detailed study of the topography of the eigenvalue problem if possible. With this goal in mind, Eversman (refs. 32 and 33) has developed an integration scheme to solve equation (58) for the circular-duct case or equation (59) for the two-dimensional-duct case. An integration scheme was used previously in connection with the no-flow case (refs. 17 to 20) and it was found, as demonstrated by equation (57), that the eigenvalue can be obtained as the solution of a nonlinear initial-value problem.

The initial-value-problem approach can be extended to the case when flow is present. The circular-duct case is discussed here. The eigenvalue problem

$$\kappa \frac{J_m'(\kappa)}{J_m(\kappa)} = -i\eta A \left(1 - M\frac{k_x}{\eta}\right)^2 = -i\eta A w^2 \tag{60}$$

with

$$\frac{k_x}{\eta} = \frac{1}{1-M^2}\left[-M \pm \sqrt{1-(1-M^2)\left(\frac{\kappa}{\eta}\right)^2}\right] = \frac{1}{1-M^2}\left(-M \pm v^{1/2}\right) \qquad (61)$$

can be transformed into a differential equation by differentiation of equation (60) and use of the Bessel equation to eliminate second derivatives of the Bessel functions. The result is

$$\frac{d}{d\varsigma}\left(\frac{\kappa}{\eta}\right) = \frac{-iw^2}{F(\kappa) + \kappa F'(\kappa) \pm 2iAM\left(w/v^{1/2}\right)(\kappa/\eta)} \frac{dA}{d\varsigma} \qquad (62)$$

where

$$F(\kappa) = -\frac{J'_m(\kappa)}{J_m(\kappa)}$$

and prime denotes differentiation with respect to the argument. In the derivation of equation (62), the admittance A is taken as a function of the nondimensional parameter ς (for $0 \leq \varsigma \leq 1$). If A_f is the admittance for which the eigenvalues are required, a simple choice is

$$A = \varsigma A_f$$

and

$$\frac{dA}{d\varsigma} = A_f$$

Equation (62) can be integrated from suitable initial conditions with $A = 0$ over $0 \leq \varsigma \leq 1$ to yield an eigenvalue of equations (60) and (61) corresponding to each starting value. It was previously shown (eq. (57)) that an initial-value problem not involving the calculation of Bessel functions can be generated in the no-flow case. This is appealing from an efficiency standpoint. It is also possible in the present case but has not been used because of adverse effects on the accumulation of error in the integration. This follows because when equation (62) is manipulated to eliminate the Bessel functions, equation (60) is used. Because the integration process at each step introduces slight errors, equation (60) is not actually satisfied exactly. This appears to have the effect of making equation (62) very sensitive, to the point of requiring extremely small integration steps.

The integration scheme employed is a fourth-order Runge-Kutta with variable step size. The step size is adjusted by monitoring the residual generated in equation (60) as the integration progresses. When an error bound is exceeded, the integration is halted and a Newton-Raphson iteration is performed to reinitialize the process. The step size is then reduced until the next integration step will lead to an error within the error bound. This type of self-correction is the exception rather than the rule, and a successful integration is often achieved with only 20 integration steps for $0 \leq \varsigma \leq 1$.

The choice of initial starting values for the integration process as the hard-wall eigenvalues seems obvious. However, when $\mathrm{Im}(A) > 0$ two additional starting values appear which lie at

$$\frac{\kappa}{\eta} = \frac{1 - M^2}{M^2} \frac{1}{A} \tag{63}$$

in the limit $A \to 0$. These starting values do not need to be imposed in the limit $A \to 0$, and in a practical calculation a slightly sharper estimate for the starting values is obtained which can be used to produce starting values of modest magnitude (ref. 33).

If the eigenvalues are ordered on the basis of increasing attenuation, the extra eigenvalues generally lie well down the list for parameters typical of turbofan engine applications. However, for low frequencies these eigenvalues can surface near the top. At least one of them has characteristics which have led some investigators to identify it as an instability mode. In fact, the appearance of these modes is not completely understood.

Finite-element, finite-difference, and weighted-residual methods also have applications in ducts with uniform flow, particularly in cases with cross sections which are not circular or rectangular or which have peripherally varying liners. These methods are also applicable when the flow is sheared and are discussed in the next section. The problem of uniform flow in a circular duct using the method of weighted residuals with trigonometric basis functions was specifically addressed in reference 23. The major advantage of any of the methods of discretization of the problem is that the resulting eigenvalue solution spans a complete finite subset of eigenvalues with neither omission nor duplication, provided the discretization is carried out to a high enough level of accuracy. On the disadvantage side, the accuracy of representation of mode shapes and eigenvalues is not uniform and generally decays with increasing modal complexity.

Sheared Mean Flow

When the mean flow is sheared, the eigenvalue problem is defined by equations (22) and (27) or equations (28) and (29). There does not appear to be any general method of obtaining closed form solutions to these equations. Several early investigators introduced approximate solutions. Pridmore-Brown (ref. 34) treated the two-dimensional case with a linear velocity gradient and with a 1/7 power profile by an approximate solution valid asymptotically under circumstances which in practical cases require a high-frequency restriction. In reference 35 a power series expansion was used, and in reference 36 a simple finite-difference discretization of the governing equations was used. This approach was based on a previously successful application of the finite-difference technique when flow is absent (ref. 37). These investigations were directed toward estimation of the attenuation in the fundamental mode. In reference 38 an exact solution within a linear shear profile was used to create an approximate effective impedance which could then have been used to treat the problem as one of uniform flow.

In order to obtain solutions with any degree of generality it is necessary to use methods of numerical solution of the governing differential equations and boundary conditions. In this section four such methods of numerical analysis are discussed.

These methods are all applicable to the simpler problems when the flow is uniform or when the flow vanishes. In most cases, however, they are not as efficient as analytic or semianalytic methods for the simpler problems, and their power is most fully realized in the sheared-flow case.

Reference 7 in the two-dimensional-duct case, reference 39 in the annular-duct case, and reference 40 in the circular-duct case used numerical (i.e., Runge-Kutta) integration of the governing equation. The integration is accomplished in terms of a transfer matrix relating the pressure and the pressure gradient at one wall to those at the other wall:

$$\begin{Bmatrix} P \\ P' \end{Bmatrix}_2 = \begin{bmatrix} T_{11} & T_{12} \\ T_{21} & T_{22} \end{bmatrix} \begin{Bmatrix} P \\ P' \end{Bmatrix}_1 \tag{64}$$

If the boundary conditions at walls 1 and 2 are represented by

$$P_1' = \epsilon_1 P_1$$

$$P_2' = \epsilon_2 P_2$$

we can write

$$\begin{Bmatrix} P \\ P' \end{Bmatrix}_1 = \begin{Bmatrix} 1 \\ \epsilon_1 \end{Bmatrix} P_1$$

$$[-\epsilon_2,\ 1] \begin{Bmatrix} P \\ P' \end{Bmatrix}_2 = 0$$

This leads to the eigenvalue equation

$$[-\epsilon_2,\ 1] \begin{bmatrix} T_{11} & T_{12} \\ T_{21} & T_{22} \end{bmatrix} \begin{Bmatrix} 1 \\ \epsilon_1 \end{Bmatrix} P_1 = 0$$

For nontrivial solutions,

$$F\left(\frac{k_x}{\eta}\right) = T_{21} + \epsilon_1 T_{22} - \epsilon_2 (T_{11} + \epsilon_1 T_{12}) = 0 \tag{65}$$

For sheared flow with no slip at the walls, T_{11}, T_{12}, T_{21}, and T_{22} are functions of k_x/η. For the no-slip case, ϵ_1 and ϵ_2 are not functions of k_x/η. The eigenvalue problem is to find values of k_x/η which satisfy equation (65).

Solutions to equation (65) are probably best obtained by a Newton-Raphson iteration with finite-difference derivatives. Several strategies can be employed to establish starting values. The most conservative approach begins with no-flow eigenvalues and a systematic incrementing of the Mach number. A second approach begins with eigenvalues for uniform mean flow but proceeds at some risk of nonconvergence in cases where the sheared flow substantially modifies the propagation characteristics.

A slightly different approach has been used in reference 41. This reference treated the case of rectangular-duct flow consisting of a central core of uniform flow and a

boundary-layer region of thickness δ. The solution for the central core can be written in analytic form. Equation (28) for the boundary-layer region is approximated by four finite-difference equations, and the interfaces at the duct-wall and boundary-layer uniform flow produce two additional finite-difference equations. The set of six homogeneous equations in terms of the unknown pressures at six finite-difference points in the boundary layer constitutes an eigenvalue equation for values of k_x/η. An advantage of this method is the elimination of the need to increase the number of integration steps for very thin boundary layers. The same number of integration points within the boundary layer is always used without complicating the solution in the uniform-flow region. Reference 41 elaborates no further on the eigenvalue solution technique, but presumably the strategy would be similar to that discussed in connection with the Runge-Kutta integration procedure (refs. 39 and 40). For the calculation of just a few eigenvalues these approaches can be reasonably efficient. However, for the determination of a large number of eigenvalues, certain techniques described in the following discussion may be less costly.

The method of weighted residuals (MWR) in the form of a Galerkin method has proven to be a powerful tool in extracting the eigenvalues for transmission through sheared flows. The Galerkin method begins with the assumption that the solution to the field equations (e.g., eq. (28)) can be approximated as a superposition of a subset of a complete set of functions $\phi_i(y)$ in the form

$$\hat{p}(y) = \sum_{i=1}^{N} q_i \phi_i(y) \tag{66}$$

where the number of basis functions N is chosen to produce convergence of the result based on the number of required accurate eigenvalues. In the standard application of the Galerkin method the basis functions are chosen to satisfy the boundary conditions. This poses no difficulty in the sheared-flow case with no slip at the wall since solutions to the no-flow problem serve the purpose.

The coefficients q_i in the superposition of equation (66) are determined in a way which minimizes the error of the trial solution. Equation (32) can be written in linear operator form as

$$\mathcal{L}[p] = 0$$

When the trial solution $\hat{p}$ is substituted, a residual, or error, results:

$$\mathcal{L}[\hat{p}] = R$$

The residual must vanish if it is orthogonal to every member of a complete set of functions. The set of test functions is chosen as the same subset of complete functions used as basis functions. Thus, N relations of the type

$$\int_0^1 \phi_j R \, dy = 0 \qquad (j = 1, 2, ..., N) \tag{67}$$

can be formed. This procedure leads to a set of N homogeneous algebraic equations for the N coefficients q_i. The coefficients in this equation depend on k_x/η and a nontrivial solution exists for discrete values of k_x/η. The algebraic equations can be cast as a linear eigenvalue problem:

$$\mathbf{Aq} = \lambda \mathbf{q} \tag{68}$$

where, depending on the structure of the particular problem, $\mathbf{A}$ is a matrix of coefficients, $\mathbf{q}$ is a vector related to the unknown coefficients in equation (66), and λ is the eigenvalue related to k_x/η. This type of eigenvalue problem is routinely solved by standard algorithms.

Hersh and Catton (ref. 42) were the first to use this procedure in the case of a hard-wall two-dimensional duct. They used the no-flow solutions in the form of trigonometric functions. They refined the estimates thus obtained by using them as initial values in the Runge-Kutta method previously described (refs. 39 and 40).

Savkar (ref. 43) approached the same problem using polynomial basis functions which were constructed to satisfy the boundary conditions for either a hard-wall two-dimensional duct or a two-dimensional duct with acoustically absorbing walls.

In references 44 and 45 the Galerkin method was used to study the attenuation in sheared flow in two-dimensional and three-dimensional rectangular ducts. This appears to be the first time this problem was cast as a linear algebraic eigenvalue problem and a large-scale eigenvalue solution routine was used. As a consequence of this approach eigenvalues were calculated which are clearly acoustic as well as eigenvalues which appear to be nearly hydrodynamic in nature. The Galerkin method was also used in references 46 and 23 in the uniform-flow case. This is a more difficult situation because the boundary condition at the wall involves the eigenvalue k_x/η. Rather than use basis functions which satisfy the boundary conditions, a boundary residual is introduced in addition to the field-equation residual. The modified Galerkin method is then used to obtain coefficients in equation (67) which minimize the field-equation residual and the boundary residual. A feature of this work is the use of the acoustic field equations in the form of the primitive variables p and V. This constitutes an application of the Galerkin method to a set of equations. The choice of basis functions is suggested by results in the no-flow case.

Yurkovich (ref. 47) demonstrated the power of the Galerkin method in his investigation of the acoustic transmission in circular and annular ducts carrying sheared and swirling flows.

The Galerkin method is but one of several methods by which the field equations and boundary conditions are replaced by discrete relations in the form of algebraic equations. Perhaps the most obvious way of doing this is by replacement of the differential equations with their finite-difference approximations. This was first proposed in reference 48. The appealing characteristic of this approach is the tridiagonal form of the difference equations. However, the structuring of the difference equations as a standard linear algebraic eigenvalue problem is hindered by the presence of the eigenvalue k_x/η in equation (22) or (28) in the coefficients of both P and P'. As shown in references 44 and 45, it is possible to replace the problem, which turns out to be cubic in k_x/η, with one which is linear in k_x/η but tripled in order. However, this would not preserve the tridiagonal character of the problem. In reference 48 an iterative scheme was devised to cope with this and to maintain a tridiagonal difference representation.

Dean (ref. 49) has also used a finite-difference scheme. He was primarily concerned with obtaining a simple eigenvalue procedure which takes advantage of the basically tridiagonal nature of the difference equations. Toward this end he replaced the

actual shear profile with a velocity discontinuity (similar to the boundary-layer displacement thickness concept). He was then able to put the entire effect of the boundary layer into the boundary condition and thus only slightly disrupt the very simple linear algebraic eigenvalue problem which would exist for completely uniform flow with a zero wall velocity. He used an iterative technique based on the nearly tridiagonal nature of the problem to calculate eigenvalues. The advantage of this over a standard algebraic eigenvalue routine is the ability to focus on specific modes without calculating the entire eigenvalue set. The disadvantage is the necessity of having good starting values and the resulting implication of convergence problems, which are analogous to difficulties found with other methods.

The most flexible of the methods of discretization of the field equations is the finite-element method (FEM). The major strength of FEM lies in the systematic treatment of problems with irregular boundaries and solution grids. The application of FEM to eigenvalue problems in ducts is relatively straightforward for circular and rectangular ducts because they are one dimensional (i.e., the transverse coordinate). No considerations of element geometry arise and one is concerned mainly with the question of choosing element shape functions which produce a good balance between eigenvalue solution accuracy and computational efficiency.

In general, in acoustic problems for ducts with attenuating walls and sheared mean flow, variational principles are not available. The finite-element formulation in duct acoustics is thus carried out with a Galerkin method and except for the choice of the basis functions and test functions is identical to the classic Galerkin method.

In the finite-element method the domain is divided into subdomains (or elements) in which suitable basis functions (or shape functions) are defined. A distinguishing feature of the finite-element method is that the shape functions interpolate the acoustic field within the element on the basis of the value of the acoustic field at discrete points (or nodes) within and on the boundary of the element. A second distinguishing feature is the fact that what is a global basis function in the classic Galerkin method is replaced in the finite-element method by a patchwork of local basis functions (shape functions) explicitly defined within each element. Continuity on interelement boundaries leads to a rationale for assembling the element "stiffness" matrices into a global stiffness matrix. The term stiffness matrix is used only by analogy with the more common applications of finite-element methods to structural analysis.

Finite-element analysis has become a field of applied mathematics in its own right. It is not appropriate, and in fact it is probably impossible within the constraints of space herein, to give the details of the applications in duct acoustics. Hence, we only refer to certain specific examples of application.

In the eigenvalue problem the application of the finite-element method is particularly simple since the field equation is an ordinary differential equation (e.g., eq. (28)) or perhaps the equivalent set of ordinary differential equations (derived from eqs. (18) and (19)). The main question to be answered is the achievable accuracy with various choices of element types. The element type relates to the geometrical shape of the element and the type of shape functions. In an ordinary differential equation the geometrical shape of the element is a straight line, so only the type of shape function is to be determined for the particular application.

Application of the finite-element method again leads to the linear algebraic eigenvalue problem (eq. (68)) for the axial wave numbers.

$$\mathbf{Aq} = \lambda\mathbf{q}$$

where λ is related to k_x/η. In this case the generalized coordinates in $\mathbf{q}$ are the values of the acoustic field at the finite-element nodes. Hence, the eigenvectors are the discrete analogs of continuous eigenfunctions which might arise from a solution of the boundary value problem of equations (22) and (27).

In the context of the eigenvalue problem for the uniform-flow duct with a general mean flow, the FEM has been investigated extensively in references 50 to 52. In the original formulation (refs. 50 and 51), elements with quadratic shape functions were used. These elements require a grid where nodal values of the acoustic state variables are specified. In certain instances the solution set of eigenvalues degenerates in accuracy rapidly as the modal order increases. Spurious eigenvalues occur with corresponding eigenvectors characterized by large slope discontinuities at element boundaries. The degeneration in accuracy is lessened by refining the mesh and thereby increasing the dimensionality of the problem.

A considerable improvement was achieved by the introduction of Hermitian elements (ref. 51). These elements, referred to loosely as "beam bending elements," have cubic shape functions based on specification of the acoustic states and their derivatives at the nodes (bending deflection and bending slope in the analogous structural element). Use of Hermitian elements eliminates spurious modes and improves the accuracy for a given dimensionality.

A second concept introduced in the improved version (ref. 51) is the equivalent of an eigenfunction expansion in vibration analysis. The eigenvalue problem for the case of mean flow is expanded in terms of a subset of the eigenvectors obtained when flow is absent. When flow is absent the eigenvalue problem is significantly reduced in dimensionality. The net effect of solving first the no-flow eigenvalue problem and then the flow eigenvalue problem with a reduced set of basis functions is to offer a considerable computational savings with minimal reduction of accuracy.

The FEM is not limited to simple geometries and can accommodate an arbitrary lining configuration, although at considerable cost in dimensionality. Reference 53 demonstrated the use of the FEM for the calculation of the eigenvalues for circular and rectangular ducts with a peripherally varying liner.

In many cases the boundary layer is thin in comparison with the duct transverse dimension. In this case a considerable simplification in the computation of the duct eigenvalues, and therefore the attenuation, can be achieved. References 54 to 56 used an asymptotic expansion within the boundary layer based on the small parameter δ/L, where δ is the boundary-layer thickness and L is the characteristic transverse dimension. This procedure produces an equivalent boundary condition to be enforced at the edge of the boundary layer. At the outer wall of a circular duct the boundary condition is

$$\frac{dP}{dr} = -\frac{(1 - M_oK)^2 \left(i\eta A + \epsilon \left\{\beta \int_0^1 \left[d\xi/(1 - M_oK\phi)^2\right] - \alpha\right\}\right)}{1 + i\epsilon\eta A \int_0^1 (1 - M_oK\phi)^2 \, d\xi} P \qquad (69)$$

where

ϵ $= \delta/R$

M_o core flow Mach number

A	wall dimensionless admittance
α	$= \eta^2 - i\eta A$
β	$= m^2 + \eta^2 k^2$
K	$= k_x/\eta$

The velocity profile in the boundary layer is given by

$$M(\xi) = M_o\phi(\xi) \qquad (0 \leq \xi \leq 1)$$

where $\xi = 1$ corresponds to the outer edge of the boundary layer. An interesting and important implication of equation (69) is the limiting case $\epsilon \to 0$, for which the boundary condition becomes identical to equation (26). thus verifying the correctness of the continuity of particle displacement assumption used in its derivation.

The boundary condition of equation (69) should be applied at the edge of the boundary layer. Since the boundary layer is assumed to be thin relative to the duct radius, it is generally adequate to apply the boundary condition at the duct wall, in which case it can legitimately be viewed as an effective admittance. Wherever applied, the effective admittance is a function of the axial wave number k_x, whereas in the usual point reacting liner boundary condition (eq. (26)) the admittance is independent of k_x (though generally dependent on η, the dimensionless frequency). In fact, the effective admittance is that of a bulk reacting boundary, that is, one that admits wave propagation.

The computation of eigenvalues can still proceed from equations (58) and (59), but the integration scheme of equations (60) to (62) is no longer directly applied. The integration scheme can be used in combination with relaxation if the eigenvalue problem is first solved with $\epsilon = 0$ (the uniform-flow case). The values of $K = k_x/\eta$ so obtained can be used to evaluate the effective admittance

$$A_{\text{eff}} = \frac{i\eta A + \epsilon\left\{\beta \int_0^1 \left[d\xi/(1 - M_o K\phi)^2\right] - \alpha\right\}}{1 + i\epsilon\eta A \int_0^1 (1 - M_o K\phi)^2 \, d\xi} \tag{70}$$

which can then be used in the integration scheme to find new values of K. This sequence proceeds to convergence of the K values. Should convergence difficulties arise, increments of ϵ can be used, but for a small ϵ this should not be necessary.

The effective admittance can be computed explicitly for linear, sinusoidal, and $1/N$ power law boundary layers. For other boundary layers the integrals may have to be computed by numerical quadrature.

Myers and Chuang (ref. 57) have improved upon the inner expansion by obtaining a uniformly valid matched asymptotic expansion which maintains accuracy for thicker boundary layers. The resulting eigenvalue problem is modified, but a similar procedure would be used to obtain eigenvalues and eigenfunctions.

General Computational Results

Design criteria for acoustic liners in turbofan inlet and exhaust ducts are considered in detail in another chapter. In this section we refer to some general results

which can be deduced. All results quoted are for tuned linings consisting of a resistive face sheet and a cavity backing. Details of lining characteristics are given in another chapter.

Rice (ref. 58) has shown that the presence of a uniform mean flow has a substantial effect on the acoustic lining impedance required to obtain maximum attenuation. For an initially planar acoustic wave introduced in a circular lined duct (constructed from the superposition of 10 nonplanar soft-wall symmetric acoustic modes), he determined the curves of equal sound power attenuation in the impedance plane, both with no flow and with an inlet flow of $M = -0.4$ (negative Mach number indicates propagation opposite to flow direction), at a nondimensional frequency $\eta = \pi$. The attenuation was computed over an axial length of 6 duct radii. The result in the impedance plane is shown in figure 3, in which it is shown that the presence of flow has a strong effect on the values of impedance which correspond to a given level of attenuation, and in particular on the impedance required to achieve optimum attenuation. He also shows that the maximum achievable level of attenuation is relatively insensitive to the mean flow. This is shown in figure 4 wherein attenuation per distance equal to duct diameter is plotted against the nondimensional frequency η. There is a substantial decrease in achievable attenuation with frequency, but very little dependence on Mach number. This result cannot necessarily be extended to other combinations of modes.

A study (ref. 26) for the two-dimensional case considered only the fundamental mode and examined the variation of the frequency at which peak attenuation occurs as a function of Mach number for specific linings. Plotted in figure 5 is the ratio of the tuning frequency f_P (frequency of peak attenuation in the fundamental mode) to the tuning frequency at zero Mach number $(f_P)_{M=0}$ as a function of Mach number. It is shown that the tuning frequency decreases in inlet flow and increases in exhaust flow. The result is relatively insensitive to the resistance of the lining.

It is found in reference 59 that modes of high spinning and radial orders (modes which are not axisymmetric) attenuate more rapidly than those of lower orders. It is concluded that some knowledge of the source is required to carry out a reasonable lining design.

The effect of the boundary layer is important in the determination of the optimum impedance. Simple considerations of ray acoustics show that for an inlet flow where the sound propagation is opposite to the mean flow, the boundary layer tends to refract acoustic rays away from the duct wall, and it might be expected that for a given lining the attenuation would be less than that calculated using a uniform mean flow. The opposite effect should occur in exhaust flows. This is supported by experiment, although a greater effect is seen in inlet flows than exhaust flows. A parametric study (ref. 60) showed that for inlet flows the optimum acoustic resistance for individual well-cut-on modes is reduced substantially with increasing boundary-layer thickness, while the boundary-layer effect on reactance is much smaller. The most significant fact found is shown in figure 6. Here the ratio of optimum attenuation with boundary layer σ to optimum attenuation with no boundary layer σ_0 is plotted against the ratio of the boundary-layer thickness δ to the wavelength λ for a given angular mode m and frequency η. For boundary layers up to 25 percent of the wavelength, the achievable attenuation is not very sensitive to the boundary-layer thickness. Hence, with proper design procedures the presence of a boundary layer need not reduce the achievable attenuation for well-cut-

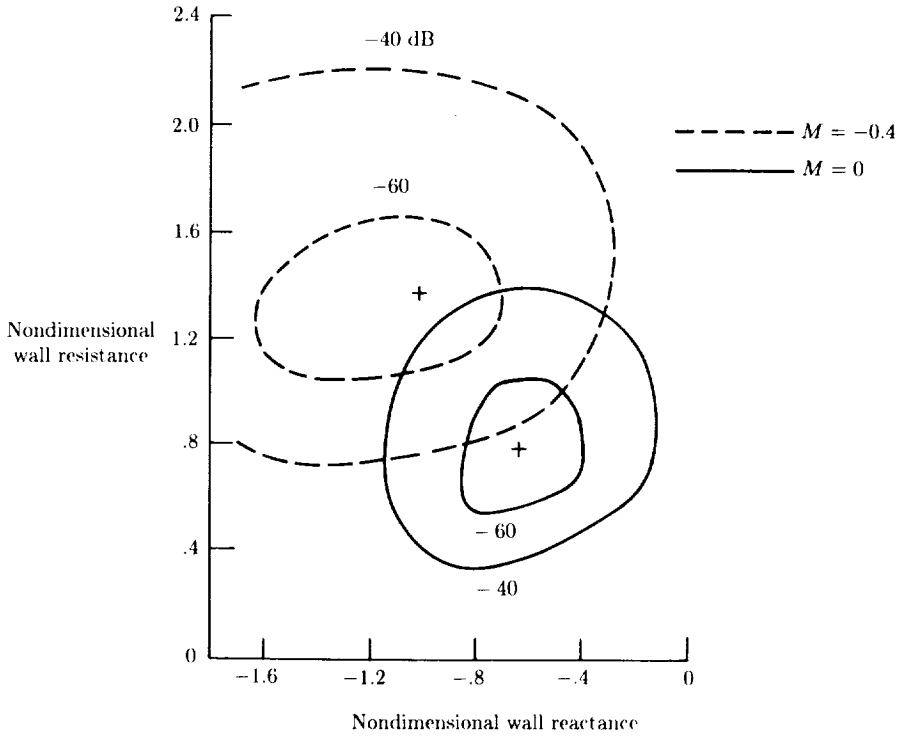

Figure 3. Contours of constant attenuation in length of 6 duct radii for circular duct. $L/D = 3; \eta = \pi$.

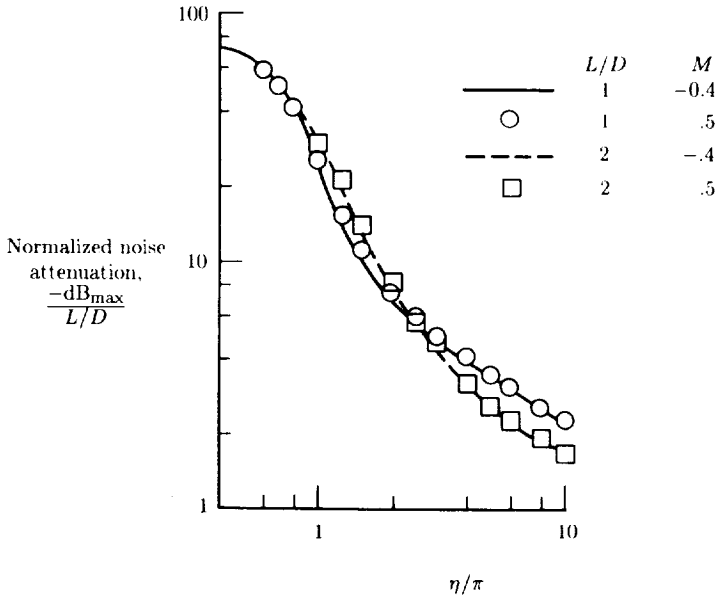

Figure 4. Maximum achievable attenuation in circular duct per axial distance equal to duct radius.

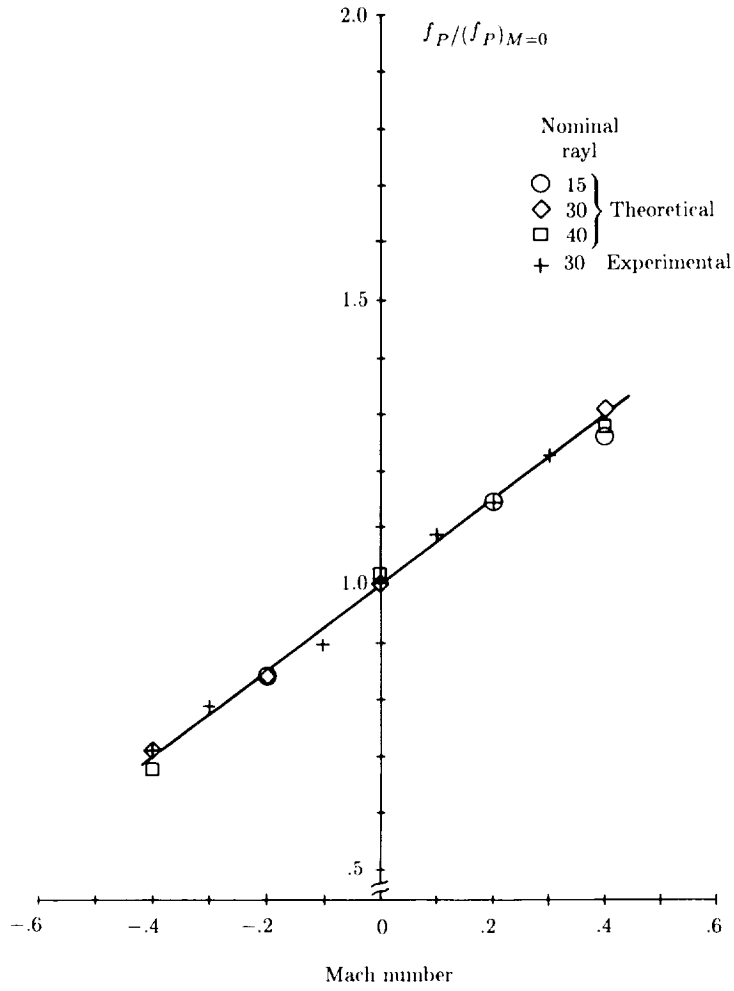

Figure 5. Comparison of theory and experiment for ratio of frequency of peak attenuation with mean flow f_P to frequency of peak attenuation without flow $(f_P)_{M=0}$ for several lining flow resistances.

on modes. This fact can be understood in the context of effective admittance. (See eq. (70).) As long as the effective admittance takes the optimal value, the attenuation is independent of boundary-layer thickness (within the limitations of the equation).

Reference 61 showed that a precise model of the boundary layer is not required to carry out practical design calculations. It showed that a boundary-layer profile which matches the shape factor (ratio of displacement thickness to momentum thickness) and the displacement thickness of the actual boundary layer produce attenuation rates essentially the same as the actual boundary layer. In particular, the 1/7 power law boundary layer can be replaced by a linear profile with slip at the wall. This observation minimizes the computational difficulties associated with sheared-flow

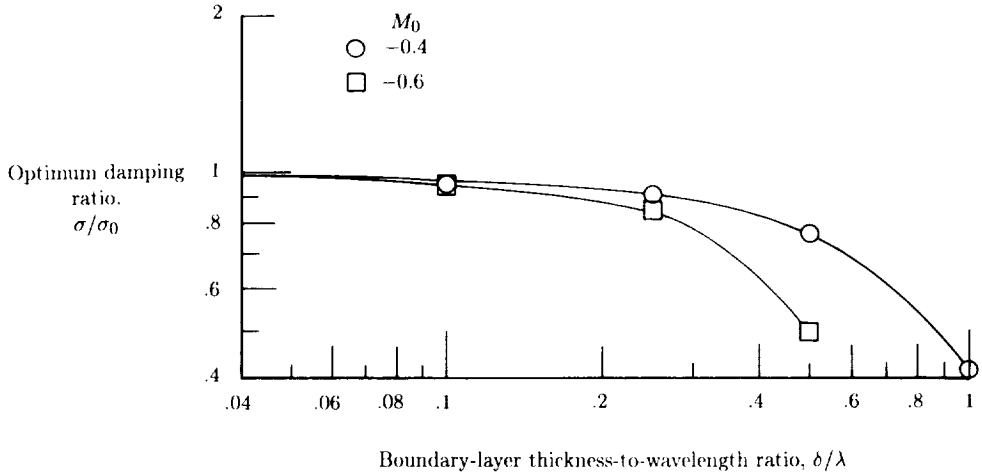

Figure 6. Effect of ratio of boundary-layer thickness to wavelength on ratio of maximum attenuation with boundary layer to maximum attenuation without boundary layer. $m = 7$ mode; $\eta = 10\pi$.

calculations. Other investigations showed that a thinner boundary layer with a linear profile but without slip can also be used to simulate the actual engine duct profiles, which are seldom of 1/7 power. If the boundary layer is not thin, care should be taken to use the actual profile.

An Alternative Calculation Scheme Based on Correlation Equations

The computation schemes introduced previously can be coupled with a suitable optimization algorithm to create a suppressor design procedure. A design iteration based on these schemes would be complicated and time-consuming and in addition may require information not available to the designer (e.g., the duct modes present). An additional complication is the large number of parameters involved, since the optimum impedance is a function of frequency, Mach number, boundary-layer thickness, and duct modes present. Furthermore, even after an optimum design is achieved (one which produces the maximum attenuation), it is necessary to consider off-design performance, which requires more analysis. In an effort to streamline this procedure, Rice (refs. 3, 59, 60, and 62 to 65) has made major contributions to the design process by identifying correlating equations from which approximate computations of suppressor performance can be made. He has found an analytic approximation for the contours of equal attenuation in the impedance plane (see fig. 3, e.g.) (refs. 62 and 63), which is a function of the optimum impedance and the optimum attenuation rate for a given mode, mean flow Mach number, boundary-layer thickness, duct geometry, and frequency. This approximation allows the rapid estimation of off-design liner performance, that is, the equal attenuation contours for linings which are not optimum.

A second major contribution to the design procedure introduced by Rice is his discovery that the optimum impedance (resistance and reactance) and the maximum

possible attenuation for a given frequency, boundary-layer thickness, and geometry are uniquely defined by the modal cutoff ratio (refs. 3 and 64). In this context, the definition of modal cutoff ratio is extended to ducts with acoustic treatment by introducing the definition

$$\beta = \frac{\eta}{R\sqrt{(1 - M^2)\cos 2\phi}} \tag{71}$$

where the axial wave number is given by

$$\frac{k_x}{\eta} = \frac{-M + \sqrt{1 - (1 - M^2)(\kappa/\eta)^2}}{1 - M^2}$$

and

$$\kappa = R \exp(i\phi)$$

Figure 7 shows the loci of optimum impedances for a given frequency, Mach number, and boundary-layer thickness. Numerical computations were carried out by Rice (ref. 3) to find the optimum impedance for a large number of modes with different spinning (angular) and radial mode numbers. The data symbols correspond to the angular mode m, and the location of the symbol around the curve clockwise corresponds to increasing radial mode number μ. Modal cutoff ratio decreases in the clockwise direction. Where two symbols are nearly coincident the modal cutoff ratios are nearly the same, as indicated by the identification of two symbols with cutoff ratios near $\beta = 1.2$.

Based on this observation reference 64 established a correlating equation for optimum impedance as a function of cutoff ratio for a given Mach number, boundary-layer thickness, and frequency. The success of the correlating equations is shown in figures 8 and 9 for a specific case. Optimum resistance and reactance are shown as a function of cutoff ratio with boundary-layer thickness as a parameter for a specific frequency and Mach number. The data symbols are the result of numerical computations and the curves are the result of the correlating equations.

Hence, algebraic equations, which result from extensive numerical analysis, insight into the theoretical results, and some empiricism, are available for the design process. Rice and Sawdy (ref. 66) have summarized the design procedure and an extension which also makes use of a correlation of the far-field directivity to cutoff ratio.

The results are based on analysis of ducts of infinite length; that is, there are no reflections from the duct termination. The results may be substantially modified for short ducts typical of fan engine inlets. The cutoff ratio remains a viable design parameter, but the duct L/D becomes an important additional parameter.

Acoustic Energy

One convenient measure of the effectiveness of acoustic treatment in a duct is the acoustic energy which is absorbed or reflected by the treatment. In principle this measure can be applied by computing the acoustic power or the acoustic energy flux (acoustic power per unit area) at two duct cross sections a distance Δx apart

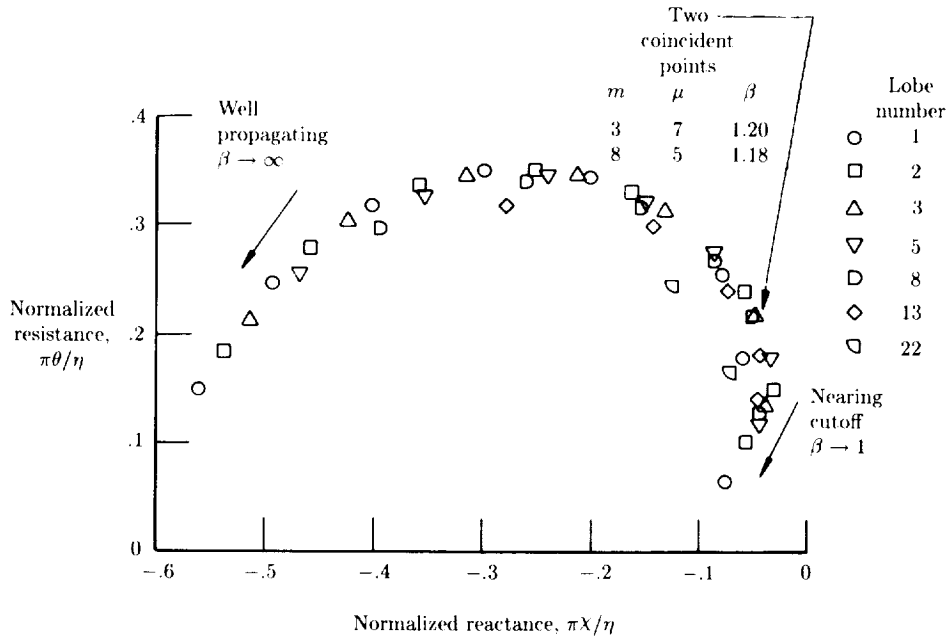

Figure 7. Loci of optimum impedance values for given frequency in circular duct with sheared mean flow. $f = 2890$ *Hz;* $\eta = 9.47\pi$; $M_0 = -0.36$; $\delta/r_0 = 0.059$.

and by then attributing the decrease in the flux to the attenuation introduced by the lining. The flux of acoustic energy can also in principle be broken down into incident, reflected, and transmitted contributions. Calculation of these components can be used to quantify the effectiveness of reactive acoustic treatment in terms of reflection and transmission coefficients.

In thermo-fluid mechanics, energy density and flux are defined in terms of products of the fluid state variables. In the acoustic case definitions of acoustic energy density and flux are to be expressed in terms of only steady-state and first-order-fluctuating acoustic perturbations. For general flows this is an elusive goal, at least in the sense of producing definitions which are appropriate for practical calculations. Morfey (ref. 67) has addressed the question of general flows, as has Möhring (refs. 68 and 69). Morfey also discussed one of two definitions of acoustic energy density and flux, which are useful for calculations in a restricted class of flows. He restricted attention to irrotational uniform entropy flow. For this case the consideration of the time-averaged flux of stagnation enthalpy across a fixed surface yields the definitions

$$E_I = \frac{1}{2\rho c^2} p^2 + \frac{1}{2}\rho V^2 + \frac{1}{c^2}(\mathbf{V}_o \cdot \mathbf{V})p \tag{72}$$

$$\mathbf{N}_I = p\mathbf{V} + \rho(\mathbf{V}_o \cdot \mathbf{V})\mathbf{V} + \frac{1}{\rho c^2}\mathbf{V}_o p^2 + \frac{1}{c^2}\mathbf{V}_o(\mathbf{V}_o \cdot \mathbf{V})p \tag{73}$$

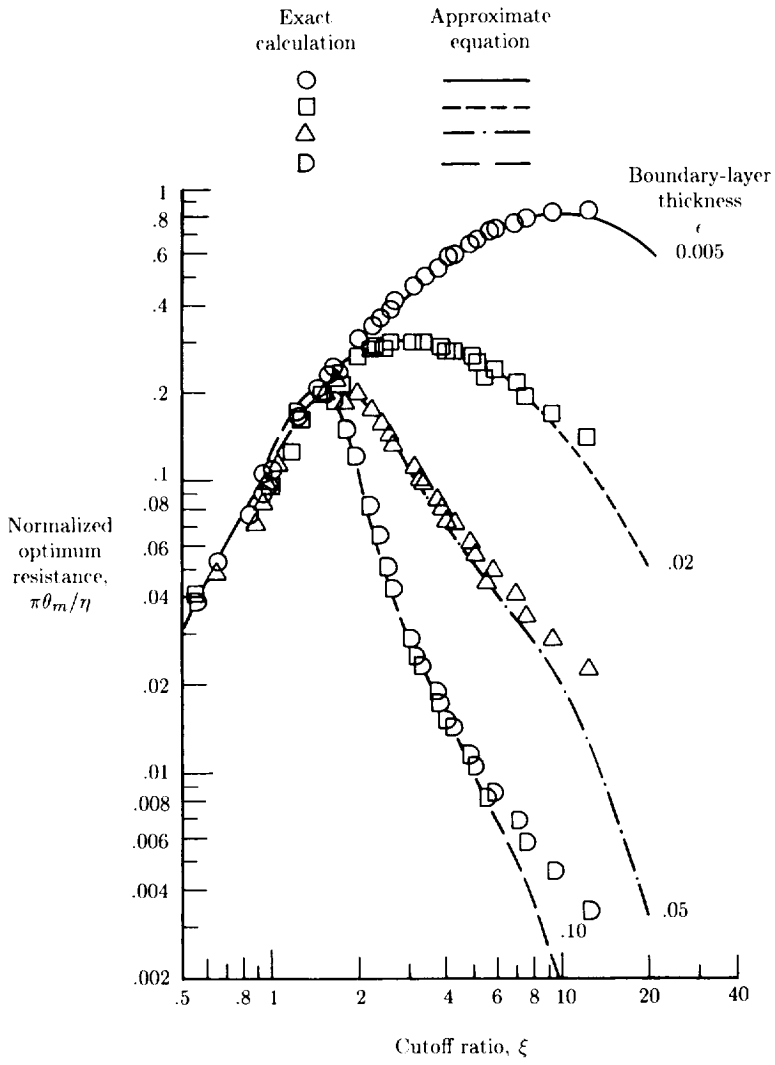

Figure 8. Comparison of correlating equation with experiment for optimum resistance for several nondimensional boundary-layer thicknesses. $\eta = 15\pi$; $M_0 = -0.4$.

where E_I is the acoustic energy density, $\mathbf{N}_I$ is the acoustic energy flux, ρ is the local mean flow density, c is the local mean flow speed of sound, and $\mathbf{V}_o$ is the mean flow velocity. These definitions are given in *dimensional* form, as is almost universally the case in the literature. The equivalent nondimensional forms are easily obtained by scaling the energy density by a suitable reference value $\rho_r c_r^2$ and the flux by $\rho_r c_r^3$. It is important to note that the definitions are entirely in terms of the steady-flow

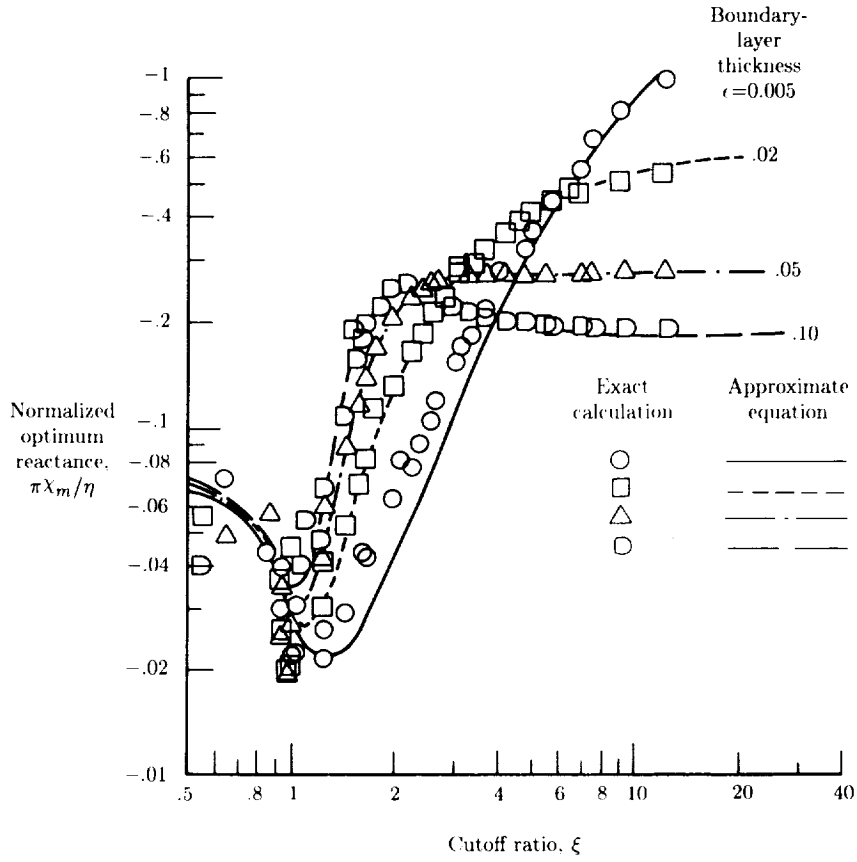

Figure 9. Comparison of correlating equation with experiment for optimum reactance for several nondimensional boundary-layer thicknesses. $\eta = 15\pi$; $M_0 = -0.4$.

state variables and second-order terms involving the first-order acoustic fluctuations p and $\mathbf{V}$.

A second approach, typified by the work in reference 70, starts directly with the thermo-fluid mechanics energy equation, expands in a perturbation series, subtracts out the steady-flow contributions, retains only second-order quantities in the acoustic fluctuations, and defines the resulting quantities as acoustic energy density and flux. If the mean flow is entirely uniform, this procedure yields the definitions

$$E_{\mathrm{II}} = \frac{1}{2\rho c^2} p^2 + \frac{1}{2}\rho V^2 \tag{74}$$

$$\mathbf{N}_{\mathrm{II}} = p\mathbf{V} + \mathbf{V}_o \left(\frac{1}{2\rho c^2}\, p^2 + \frac{1}{2}\rho V^2 \right) \tag{75}$$

These are again in terms of second-order terms involving the first-order acoustic fluctuations.

The acoustic intensity in either case is defined as the time-averaged acoustic energy flux

$$\mathbf{I} = \langle \mathbf{N} \rangle$$

The total acoustic power at a duct cross section is

$$P = \int \int_S \mathbf{I} \cdot \mathbf{n} \, dS$$

where S is the surface area over which the integral is carried out. If there are no energy sources or sinks the acoustic power is conserved between two duct cross sections Δx apart. This result is true for both definitions of acoustic energy flux.

Candel (ref. 71) has reviewed much of the literature dealing with acoustic energy principles in general and their application to ducts in particular. The classification given herein is consistent with his observations. Both forms are valid sets of definitions, but the type I energy definitions satisfy a conservation law for a wider class of flows.

Eversman (ref. 72) shows that the two forms of energy density are compatible with variational principles, from which the acoustic field equations can be derived in the case of uniform flow when both definitions satisfy a conservation law. The term E_{I} is the Hamiltonian density and E_{II} is the Lagrangian density. In general, $E_{\mathrm{I}} \neq E_{\mathrm{II}}$ and $\mathbf{N}_{\mathrm{I}} \neq \mathbf{N}_{\mathrm{II}}$. However, this is not significant; as energy-related quantities, suitable additive constants can be introduced to force equivalence. The important fact is that the change in acoustic power between two duct cross sections Δx apart is zero when no energy sources or sinks are present.

When energy sources or sinks are present, a modified form of the definition of acoustic power must be used to account for them. This has been done for a lined uniform duct with uniform flow (ref. 72). The appropriate definitions are

$$P_{\mathrm{I}} = \int \int_S \langle \mathbf{N}_{\mathrm{I}} \rangle \cdot \mathbf{n} \, dS + V \left(\langle p_b \varsigma \rangle + pV \langle u_b \varsigma \rangle \right)$$

$$P_{\mathrm{II}} = \int \int_S \langle \mathbf{N}_{\mathrm{II}} \rangle \cdot \mathbf{n} \, dS + V \int \left\langle p_b \frac{\partial \varsigma}{\partial x} \right\rangle dx$$

The surface integral terms are recognized as the power definitions for the hard-wall duct. The terms p_b and u_b are the values of the acoustic pressure and the axial component of the acoustic particle velocity at the duct wall. The term $\varsigma(x,t)$ is the wall displacement field. It is found that

$$\frac{dP_{\mathrm{I}}}{dx} = \frac{dP_{\mathrm{II}}}{dx} = -\langle r_b \varsigma_t^2 \rangle$$

where r_b is the resistive component in the lining impedance,

$$Z = \frac{P}{\varsigma_t} = r_b + i x_b$$

and ς_t is the normal component of velocity at the wall. Hence, the rate of decrease of acoustic power is the same for either definition.

Nonuniform Ducts

The duct system through which fan noise propagates and radiates is contoured for aerodynamic and propulsive efficiency. In the acoustic design sequence it may be necessary to determine the effect of the duct nonuniformity on the lining performance. Modeling of acoustic propagation in the fan inlet and exhaust ducts involves consideration of the geometric nonuniformity of the duct as well as the resultant nonuniformity in the mean flow. The problem thus becomes one of considerable complexity for which no "exact" analytical solution is generally available, as in the case of many comparable problems in uniform ducts.

As noted previously, the propagation and radiation problems are coupled and should be solved simultaneously. This is the ultimate goal of the modeling process. However, most analysis methods have approached the propagation and radiation problems separately by treating the propagation as occurring in a duct with no reflection at the termination and the radiation then proceeding from the conditions established in this manner at the termination. Even this simplification leaves the difficult problem of describing the mean flow in the duct and the acoustic propagation in the presence of this flow.

In this section we look at methods which have been used to consider the acoustic propagation in nonuniform ducts with reflection-free terminations. This challenging problem was first attacked for the case when the mean flow vanishes or can be assumed to be of negligible effect. Subsequent extensions were made to include the effect of mean flow. The discussion herein is split up in the same way and a number of techniques are reviewed.

The question of radiation to the far field is addressed in the final section of this chapter, wherein modeling methods are introduced with which the entire propagation and radiation process can be described. This section and the final one are thus closely related.

Nonuniform Ducts Without Mean Flow

Methods of modeling linear acoustic propagation in nonuniform ducts without flow can be broken down into five major categories: (1) one-dimensional or plane-wave approximations; (2) approximations for higher order acoustic modes which neglect modal coupling; (3) stepped duct approximations; (4) variational and Galerkin methods; and (5) finite-element and finite-difference methods. The last category of methods has been successfully extended to include the radiation to the far field.

At low frequencies the Webster horn equation (ref. 73) can be obtained either by directly considering one-dimensional forms of the continuity and momentum equations or by expanding the acoustic equations in terms of powers of a small parameter which is the ratio of the duct radius to the wavelength. The first-order terms are the Webster equation. The resulting theory is equivalent to the "plane-wave theory" in uniform ducts. For most problems in turbofan duct acoustics the theory is not adequate for the representation of high-frequency propagation from rotating-blade noise sources. However, the solution of Webster's equation has been used in a modern context in reference 74 in connection with studies of the acoustic properties of the contoured circular duct present in a bottle neck.

When the cross-sectional area of the duct or the acoustic lining properties vary slowly, perturbation techniques become useful. The method of multiple scales was used in reference 75 in connection with the acoustic wave equation in the case without mean flow to represent the propagation of a single mode. To this level of approximation no interaction can occur between the various acoustic modes which occur in the duct. A second approach, which arrives at essentially the same result in the case of the duct with no acoustic lining, comes from reference 76. It used a Galerkin method but neglected the modal interaction in an application of the WKB approximation for the resulting uncoupled set of ordinary differential equations with slowly varying coefficients. The result is a solution for the axial variation of amplitude of the acoustic modes in the duct, but without the effect of modal interaction.

A reasonable approach to the modeling of a nonuniform duct which includes the effects of modal interactions is the segmentation of the duct into a sequence of uniform ducts with step changes in duct cross-sectional area or lining impedance at the interfaces. It is assumed that in each segment the pressure field can be approximated by a finite (and hopefully small) number of the acoustic modes for the section, each with undetermined amplitude. Conditions of continuity of mass and axial momentum at the interfaces are enforced in that a sequence of residuals, weighted by the acoustic modes themselves, are required to be orthogonal on the cross sections of the discontinuities. For given input modal amplitudes and an assumed reflection-free termination, it is possible to set up a set of linear equations for the modal amplitudes in each segment. Acoustic pressures at any point in the duct can then be recovered by suitable postprocessing of the modal amplitudes and associated acoustic modes. In reference 77 this method was introduced for the uniform duct with an axially varying lining, and it was used in reference 78 for the case of a duct with axially varying cross-sectional area. It is appropriate to point out here that the segmentation approach has also been employed in the case of ducts with mean flow. Axially segmented linings in a uniform duct with uniform flow were considered in reference 79 and extended to shear flows in reference 80.

The first use of a Galerkin method (or, more generally, the method of weighted residuals (MWR)) in the duct acoustic propagation problem was apparently in reference 76, as previously noted. This investigation of hard-wall ducts was based on a velocity potential. The formulation admitted the effect of modal coupling, but this was subsequently neglected at the solution stage. We are interested in the more general case when modal coupling effects are retained and a locally reacting duct liner is present.

The application of the Galerkin method to propagation in nonuniform ducts is similar to the application to the eigenvalue problem described by equations (66) to (68). Figure 10 shows the general geometry of the nonuniform duct between semi-infinite uniform ducts. In the nonuniform section $0 \leq x \leq L$, the impedance $Z_B(x)$ and the area $S_B(x)$ can vary. This figure can be considered either as a two-dimensional or circular duct (θ = Constant plane in a cylindrical coordinate system).

The acoustic field is described by field equations, represented here by a linear vector operator $\mathcal{L}_F$, acting on the acoustic state variables, which may include pressure p and particle velocity $\mathbf{V}$:

$$\mathcal{L}_F[\mathbf{V}, p] = 0 \tag{76}$$

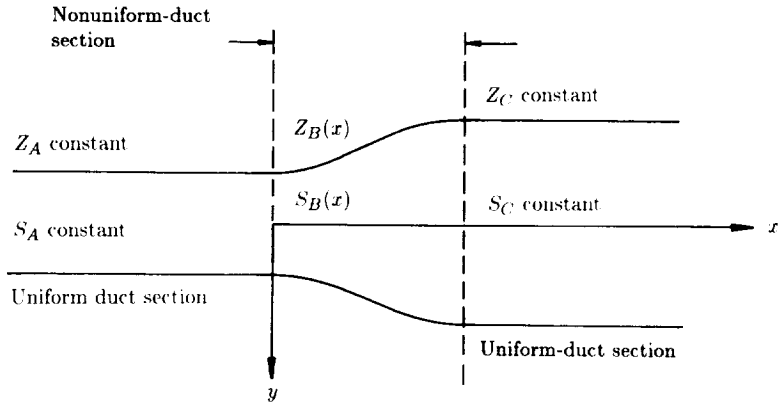

Figure 10. Geometry of nonuniform-duct segment between uniform infinite ducts.

The term $\mathcal{L}_F$ is written as a vector operator because it may represent several field equations. For example, equation (76) could be the acoustic continuity and momentum equations (eqs. (18) and (19) with $M = 0$) in the case of harmonic motion,

$$i\eta p + \nabla \cdot \mathbf{V} = 0 \tag{77}$$

$$i\eta \mathbf{V} = -\nabla p = 0 \tag{78}$$

or it could be the Helmholtz equation in pressure only:

$$\nabla^2 p + \eta^2 p = 0 \tag{79}$$

Solutions are sought in the form of a superposition of the transverse acoustic modes for a duct which is locally uniform:

$$\{P\} = [\phi]\{q\}$$

where $\{P\}$ is the vector of field variables (for example, three components of particle velocity and pressure), $[\phi]$ is a suitable modal matrix derived for a locally uniform duct, and $\{q\}$ is the vector of modal amplitudes (generalized coordinates).

The uniform-duct acoustic modes do not satisfy the boundary conditions for the nonuniform duct, and these conditions must be included as part of the problem statement. On the duct wall,

$$\mathbf{V} \cdot \boldsymbol{\nu} = \boldsymbol{A}p$$

This can be cast as the following boundary operator:

$$\mathcal{L}_B[\mathbf{V}, p] = 0 \tag{80}$$

The assumed solution $\{P\}$ is substituted in both the field equation operator and the boundary operator and produces errors, or residuals, as follows:

$$\mathbf{R}_F = \boldsymbol{\mathcal{L}}_F[\{P\}] = \boldsymbol{\mathcal{L}}_F\Big[[\phi]\{q\}\Big] \tag{81}$$

On the boundary,

$$\mathbf{R}_B = \mathcal{L}_B[\{P\}] = \mathcal{L}_B\Big[[\phi]\{q\}\Big] \tag{82}$$

For the Galerkin method (ref. 81), the residuals are required to be orthogonal to each member of a complete set, in this case the acoustic modes (basis functions) themselves, thus establishing a set of ordinary differential equations for the elements of the modal amplitude vector $\{q(x)\}$ which by implication tend to produce zero residual error. The statement of orthogonality is

$$\int_0^\sigma [\phi]^T \boldsymbol{\mathcal{L}}_F\Big[[\phi]\{q\}\Big]\, dy = 0 \tag{83}$$

On the boundary,

$$[\phi]^T \mathcal{L}_B\Big[[\phi]\{q\}\Big] = 0 \tag{84}$$

In carrying out the integration equation (83), it is found that boundary terms arise which can be eliminated with the boundary residual. This is the equivalent of natural boundary conditions in variational methods.

The set of differential equations arising from the Galerkin procedure is of the form

$$\left\{\frac{dq}{dx}\right\} = [B]\{q\} \tag{85}$$

A transfer matrix relating $\{q(0)\}$ and $\{q(L)\}$, the values of the amplitudes at $x = 0$ and $x = L$, is readily obtained by a numerical integration scheme (e.g., the Runge-Kutta scheme):

$$\{q(L)\} = [T]\{q(0)\}$$

The terms $\{q(L)\}$ and $\{q(0)\}$ can then be expressed in terms of incident and reflected acoustic modal amplitudes in the uniform sections (lined or unlined):

$$\{q(0)\} = [A(0)]\begin{Bmatrix} a^+ \\ a^- \end{Bmatrix}$$

$$\{q(L)\} = [A(L)]\begin{Bmatrix} b^+ \\ b^- \end{Bmatrix}$$

where $[A(0)]$ and $[A(L)]$ are suitable matrices for the known modal structure of incident and reflected waves at $x = 0$ and $x = L$. It is then possible to establish a transfer matrix in the form

$$\begin{Bmatrix} b^+ \\ b^- \end{Bmatrix} = [TA]\begin{Bmatrix} a^+ \\ a^- \end{Bmatrix}$$

This can be decomposed under the assumption that the incident modal amplitudes $\{a^+\}$ are known and that the duct termination is reflection free ($\{b^-\} = 0$) to define reflection and transmission coefficients. The reflection and transmission coefficients can be used in a postprocessing operation to construct the acoustic field in the nonuniform section.

The MWR was used in reference 82 for two-dimensional ducts. Reference 83 used what is essentially a MWR in connection with a "wave-envelope" representation of the acoustic state variables (in this case pressure only) to treat the same problem. The wave-envelope approach isolates the rapidly varying wave structure of the acoustic propagation from relatively slowly varying changes in the modal amplitudes in order to create a set of ordinary differential equations analogous to equations (83) and (84) but which represent the relatively slow amplitude variations. Advantages can be expected in the resolution required in the integration scheme.

The finite-element method offers a much more flexible scheme than the MWR for modeling the acoustic transmission properties of nonuniform-duct segments. As noted previously, in applications in acoustics it is generally most appropriate to base a finite-element approximation on the Galerkin method. When this is accomplished, equation (85), which is a set of ordinary differential equations for the modal amplitudes, is replaced by a set of algebraic equations for the acoustic state variables at the finite-element nodes. In a manner completely analogous to the one used in the classic Galerkin scheme, the finite-element representation in the nonuniform section can be matched to a modal representation in the semi-infinite entrance and exit ducts. The result of these operations is a large set of algebraic equations of the form

$$[K]\begin{Bmatrix} \{P\} \\ \{a^-\} \\ \{b^+\} \end{Bmatrix} = [F]\{a^+\} \tag{86}$$

where the elements of the vector $\{P\}$ are the acoustic state variables at the finite-element nodes in the nonuniform section. The term $\{a^-\}$ is a vector of reflected modal amplitudes in the inlet semi-infinite duct, $\{b^+\}$ is a vector of transmitted modal amplitudes in the exit semi-infinite duct, $\{a^+\}$ is a vector of specified incident modal amplitudes in the inlet semi-infinite duct, $[K]$ is the assembled "stiffness" matrix; and $[F]\{a^+\}$ is the generalized "force" vector. An appropriate solution of equation (86) yields the reflection and transmission matrices

$$\{a^-\} = [R]\{a^+\}$$

$$\{b^+\} = [T]\{a^+\}$$

With modern finite-element schemes the large set of equations does not actually need to be stored in active computer memory. "Frontal methods" (ref. 84) provide a systematic scheme in which the finite-element assembly process and the equation solving are integrated into an algorithm which requires only a modest active memory, almost independent of the problem size. There is a vast amount of literature on finite-element methods in general, and two particularly well-known works are references 85 and 86.

The use of the finite-element method in the absence of mean flow is discussed in references 87 to 91 in connection with the modeling of mufflers, a physical arrangement not significantly different from the fan inlet problems of interest here. Craggs' work (refs. 90 and 91) was somewhat unique in that he was interested in modeling truly three-dimensional geometries (as opposed to the more widely discussed two-dimensional or axisymmetric problems), and therefore he discusses three-dimensional elements. Tag and Akin (ref. 92) made calculations for a two-dimensional nonuniform duct. All these investigations were based on a variational formulation, requiring some manipulations which are not required when a Galerkin method is used. The chief difference in the approaches is in the specific elements used.

Reference 93 presents a comparison of the use of the method of weighted residuals and the Galerkin finite-element method for the calculation of the transmission and reflection properties of acoustically treated nonuniform ducts. The finite-element method produces virtually exactly the same results for reflection and transmission coefficients as does the standard Galerkin method. The computational cost of the finite-element method when based on the Helmholtz equation is about the same as the comparable Galerkin solution. The formulation in reference 93 is the only one which employs the matching of the finite-element solution in the nonuniformity to a modal solution in the inlet and exhaust semi-infinite ducts. This, or an equivalent approach, is essential to adequately account for inlet and exhaust boundary conditions in the finite-element solution.

Finite-difference methods have also been extensively studied for application to the duct acoustics problem. Time-dependent (transient) and harmonic steady-state formulations have been used, and implicit and explicit schemes have been tested. While good results in relatively simple test cases have been reported, the finite-difference method has not become a generally used computational scheme. The main reason is the penalty imposed on finite-difference schemes by irregular geometries. Finite-element schemes are particularly well suited for duct problems, especially when nonuniform ducts are considered and when the question of imposing meaningful forcing and termination conditions is raised. It might also be added here that the finite-element scheme is more suitable for modeling the radiation to free space when this type of boundary condition is appropriate. A complete review of finite-difference applications in duct acoustics has been made by Baumeister (ref. 94), who has also made a number of contributions in this area. Consult this review for further details.

A comparison of experiment to theory for a simple nonuniform-duct geometry was reported in reference 95. Both the finite-element theory of reference 93 and the finite-difference calculations of White (ref. 96) were found to be in good agreement with the experiments.

Nonuniform Ducts With Mean Flow

Two types of nonuniform ducts are considered. The simplest situation is that of a duct of uniform cross section but with axially varying lining impedance. In this case the mean flow is axially uniform. This problem has been of considerable interest in connection with the design of linings which are segmented axially with the two objectives of providing attenuation over a broad range of frequencies and of inducing attenuation because of the reactive effects of lining discontinuities. As previously noted the stepped duct approximation (also referred to as mode matching) is suitable

for modeling transmission in a duct with segmented linings, even in the presence of sheared mean flow. Reference 79 for ducts with uniform flow and reference 80 for sheared mean flow have used the mode matching technique.

When a duct area nonuniformity is present, we are concerned not only with the effect of the area nonuniformity on the propagation, but also with the effect of the axial and transverse flow gradients induced by the area nonuniformity. A limiting case would be the situation in which the area nonuniformity creates a sonic flow at the throat, completely cutting off upstream transmission. Experimental investigations of this attenuation mechanism in references 97 to 99 have shown that locally sonic flow conditions in an inlet can create a substantial reduction in the forward transmission of fan-generated noise, although the noise cannot be completely suppressed. Perhaps of even more interest is the observation that the mechanism appears to be at least partially effective for throat Mach numbers below sonic, perhaps as low as 0.8. An effort to determine whether linear acoustic analysis could predict this flow-induced attenuation led to a substantial effort to model propagation through high subsonic flows.

A complicated situation occurs when the duct is nonuniform in cross section. We also include the possibility that the lining is axially nonuniform. It is necessary not only to model propagation in the nonuniform geometry, but also to consider the effect of propagation through the nonuniform flow field. In general, the mean flow is computed separately and is given as data for the acoustic analysis. The model used for the mean flow has substantial influence on the complexity of the acoustic model. If no restriction is placed on the mean flow and it is allowed to be rotational (principally due to the duct-wall boundary layers), then an appropriate form for the acoustic field equations is the acoustic momentum equation and the acoustic energy equation (eqs. (6) and (7)). An alternative is the acoustic field equations derived directly from the continuity and momentum equations (1) and (2). This type of mean flow representation has to be obtained from the Euler equations or the Navier-Stokes equations. If the mean flow is irrotational, then the acoustic field equations can be obtained in the form of equations (9) and (11). This means that the mean flow must be nonviscous and that no boundary layer can be included.

The computational implications of the two representations are substantial. If the mean flow is assumed to be general, then it is necessary to work in terms of the primitive variables pressure (or density) and velocity, with four field equations for three-dimensional acoustic fields. If the mean flow is assumed to be irrotational, then the acoustic field is also irrotational and the introduction of an acoustic velocity potential leads to only one field equation for the potential. The acoustic pressure and particle velocities are obtained by postprocessing the velocity potential solution.

When there is mean flow present, the boundary condition at duct hard walls is still the requirement that the normal component of acoustic particle velocity must vanish:

$$\mathbf{V} \cdot \boldsymbol{\nu} = 0$$

When a mean flow is present in a uniform duct, it was shown in equation (26) that for a locally reacting lining within a circular duct the boundary condition is

$$\mathbf{V} \cdot \boldsymbol{\nu} = Ap - \frac{iM}{\eta} \frac{\partial}{\partial x}(Ap) \tag{87}$$

In this form the boundary condition is valid for a lining which varies axially. In the case of a nonuniform duct and nonuniform mean flow, it is shown in reference 100 that the correct boundary condition is

$$\mathbf{V} \cdot \boldsymbol{\nu} = Ap - i\frac{V_\tau}{\eta}\frac{\partial}{\partial \tau}(Ap) + i\frac{Ap}{\eta}[\boldsymbol{\nu} \cdot (\boldsymbol{\nu} \cdot \nabla)\mathbf{V}_o] \tag{88}$$

where V_τ is the tangential component of mean flow $\mathbf{V}_o$ at the duct wall. The derivative $\partial/\partial\tau$ is with respect to the curvilinear distance along the duct wall. Equation (88) is directly obtained from equation (87) by replacing the axial coordinate x with the tangential coordinate τ and adding the last term. In duct applications the extra term in equation (88) is probably extremely small, since its principal contributions are only large near a stagnation point in the mean flow. Equation (87) is therefore taken as the appropriate boundary condition.

There are fewer options available for computations of acoustic propagation in ducts with nonuniform cross sections with mean flow than for comparable problems without mean flow. They can be categorized as (1) one-dimensional or plane-wave approximations, (2) perturbation schemes for ducts with slowly varying cross sections, (3) weighted-residual methods (i.e., Galerkin), and (4) finite-element and finite-difference methods.

A particularly useful one-dimensional model for unlined ducts has been constructed in reference 101 from a one-dimensional continuity and momentum equation. Without flow the governing equations can be combined to form Webster's horn equation. In their investigation they used a shooting technique to investigate the two-point boundary value problem for wave propagation in a nonuniform duct carrying a compressible mean flow with specified driving and exit conditions. The present author has used the field equations of Davis and Johnson with a Runge-Kutta integration scheme matched to traveling wave solutions in semi-infinite uniform inlets and pipes to construct transmission and reflection equations for long-wavelength propagation. Though unpublished, this approach was used as a check on a more general Galerkin formulation to be discussed shortly. King and Karamcheti (ref. 102) obtained solutions to what is effectively the Davis and Johnson model using the method of characteristics.

Perturbation methods have been used by several investigators for studies of acoustic transmission in nonuniform ducts with mean flow. In reference 103 a ray acoustics approximation was used for the velocity potential for the lowest order mode described by a generalization of Webster's horn equation. Tam (ref. 104) used a Born approximation based on a small area variation and studied the scattering of an acoustic wave incident on a nonuniformity. His flow model was constructed from the one-dimensional gas dynamics relationships with a superposed transverse velocity to create flow tangency at the walls. References 105 and 106 extended the method of multiple scales (ref. 75) to include the case with a sheared mean flow in a lined duct.

It is difficult to draw general conclusions from these models. However it can be stated that little scattering effect is seen for acoustic waves incident upon a nonuniformity (and, hence, axial and transverse flow gradients) unless the local Mach number exceeds 0.6. For higher throat Mach numbers, scattering becomes significant (ref. 104). For propagation against the mean flow, an increase in acoustic pressure near the throat is observed, the increase being very large for high subsonic

throat Mach numbers. Even for near-sonic throat velocities no large attenuation is observed.

These analytic, or semianalytic, approximations have obvious limitations implied in the perturbation schemes. In order to relax these restrictions it is necessary to resort to the Galerkin methods or to finite-element or finite-difference schemes.

The application of a Galerkin method or a finite-element analysis to the case when a mean flow is present is formally the same as when there is no mean flow. The field equations are considerably more complex, meaning that much more time is required in the computation of the coefficient matrices in the Galerkin method and of the element "stiffness matrices" in the finite-element analysis. The actual solution of the ordinary differential equations in the Galerkin method or of the algebraic equations in the finite-element analysis is neither more time-consuming nor more storage dependent than the corresponding operations when flow is absent, provided that the same level of discretization is used. In actual computations for high subsonic mean flows, it is found that upstream of the sound source the compression of the acoustic wavelengths requires a finer discretization than in the no-flow case. Downstream of the source the opposite is true. On balance, however, it appears that a finer discretization is required when flow is present.

Acoustic transmission in nonuniform ducts with a general mean flow has been considered in references 46 and 52. In reference 46 the Galerkin method was used with basis functions derived from a uniform-duct analysis, and in reference 52 a Galerkin finite-element analysis was used. The mean flow is derived from one-dimensional compressible flow relations with a simple superposition of a transverse velocity component based on the requirement of flow tangency at the wall. This is essentially the representation of the flow used in the perturbation solution of reference 104. The techniques of references 46 and 52 give comparable results and compare well with computations based on the reference 101 formulation at low frequencies.

Reference 107 extended the wave-envelope method (ref. 83) to the case of nonuniform lined ducts carrying a compressible, sheared mean flow. As previously noted this method is basically a weighted-residual, or Galerkin, approach with the refinement that the harmonic wave character of the solution is included in the basis functions so that only the envelope of the axial variation of the acoustic modal amplitudes is numerically computed. This would appear to have some implications in the efficiency of the axial integration scheme.

The weighted-residual computational schemes have been used to shed further light on the question of attenuation in propagation through high subsonic mean flows. Results were shown in reference 46 for the transmission of initially planar two-dimensional waves through a converging-diverging nozzle at low frequency, and the results were compared with equivalent one-dimensional calculations based on the formulation in reference 101. One example was a converging-diverging hard-wall duct with propagation opposite to the flow. The duct throat height was 75 percent of the inlet and exit duct heights and the nonuniform section was 1.25 duct heights in length. Mach numbers of 0.25, 0.60, and 0.81 in the throat were considered (0.20, 0.40, and 0.48 in the uniform sections). Figure 11 is a plot of the ratio of transmitted acoustic power to incident acoustic power for nondimensional frequencies based on the duct height H_1. (This is actually half the duct height if the straight wall is construed as a centerline.)

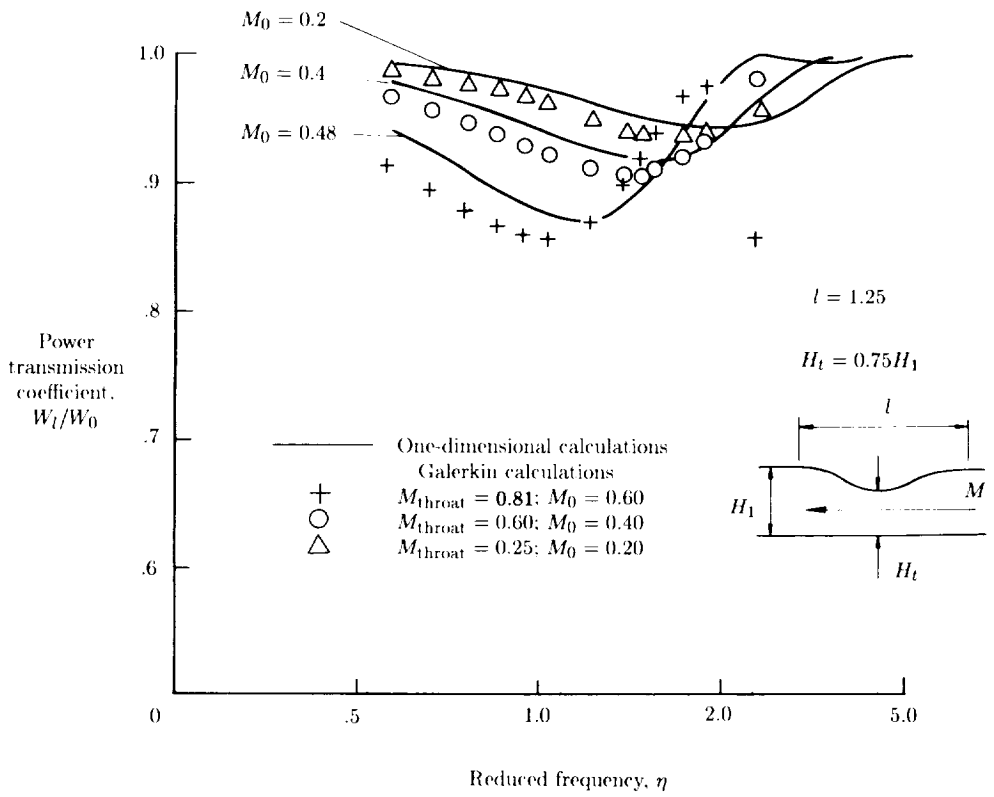

Figure 11. Ratio of transmitted power W_l to incident power W_0 in converging-diverging hard-wall duct showing comparison of one-dimensional results and Galerkin calculations.

The comparison of the one-dimensional and weighted-residual (Galerkin) results is good up to the frequency where the first higher order mode cuts on. Slight deviations occur because the weighted-residual model is inherently two dimensional, and even at low frequencies some two-dimensional effects occur. Of more interest for the present discussion is the fact that strong acoustic attenuation does not occur. What little attenuation that is shown in figure 11 is in a narrow frequency band and is the reactive attenuation of the duct nonuniformity acting as a muffler. This supports the previous observation that linear theory does not appear to predict the experimentally observed attenuation in high subsonic flows.

When the flow field can be assumed to be irrotational, the field equations become particularly simple. The continuity equation (9) and the version of the acoustic momentum equation (11) are in a form well suited for finite-element analysis. In references 108 and 109 these equations were effectively combined and a finite-element discretization was carried out based on the "wave-like" equation which results. The mean flow was generated from a boundary-element method for incompressible potential flow. A well-known compressibility correction (ref. 110) was then used to include the major effects of the compressible mean flow. Boundary conditions,

including the effect of acoustic lining, were forced on the global "stiffness" matrix. No attempt was made to match the solution in the nonuniformity region to incident- and reflected-wave structures at the terminations. The treatment of the termination conditions limits the practical application of the scheme.

When the mean flow is general and not restricted by the assumption of irrotationality, the field equations cannot be combined into a single scalar equation. Finite-element modeling schemes have been set up in references 52 and 111 for this type of flow, with the field equations in the form of equations (6) and (7) (in ref. 52) or in the form of equations (5) and (6) (in ref. 111). There are considerable differences in the details of the implementation of the Galerkin finite-element scheme. Two-dimensional flow was considered in reference 52, and natural boundary conditions were used for the duct-wall boundary conditions. A modal matching procedure was used to match the finite-element solution for the nonuniformity to the infinite inlet and exhaust ducts. This is a direct extension of the formulation for no flow (ref. 93). Reference 111 originally used forced boundary conditions, including the specification of acoustic pressure on the source plane and a modal impedance on the exit plane. In subsequent development of this scheme, modal boundary conditions were incorporated at the duct terminations. This work was directed toward the development of a very-large-scale, general-purpose duct acoustic computational scheme and was set up for axisymmetric propagation.

Finite-element methods have been shown to produce results in good agreement with results from other available computational schemes. Reference 111 shows excellent agreement with some analytic solutions. Figure 12, taken from reference 52, shows the power transmission coefficient as a function of the nondimensional frequency based on duct semiheight for the Galerkin method and for the finite-element method. The geometry is a converging two-dimensional, lined, cosine-shaped tapered-duct section with a 15-percent contraction. The propagation is against the flow, which is relatively low at $M = 0.36$ in the minimum area. The comparison of the two calculations is very good.

Finite-difference schemes, though placed on a firm foundation in reference 94, have not become generally useful. This is undoubtedly because of the simplicity with which finite-element schemes handle complicated geometries. A second consideration is the introduction of frontal solution schemes in the finite-element method which put these methods on a nearly equal footing with explicit finite-difference algorithms when computer storage is a consideration.

Radiation

It has been noted previously that duct acoustic propagation and radiation are coupled and cannot be separated in a rigorous treatment. It has also been noted that most duct propagation analysis has been carried out by ignoring the radiation aspect. The usual way to avoid it is to assume that the duct is of infinite length and that the reflection effects at the termination are unimportant. This effectively says that the radiation process proceeds on the basis of conditions established at the duct termination by propagation without reflection, and therefore the radiation process creates no reflections. For lining design this has proven to be an effective approach, since reflections are relatively unimportant except at frequencies near modal cutoff.

When the radiation pattern itself is of interest, then the problem of acoustic radiation in the infinite medium surrounding the duct exit must be addressed. In

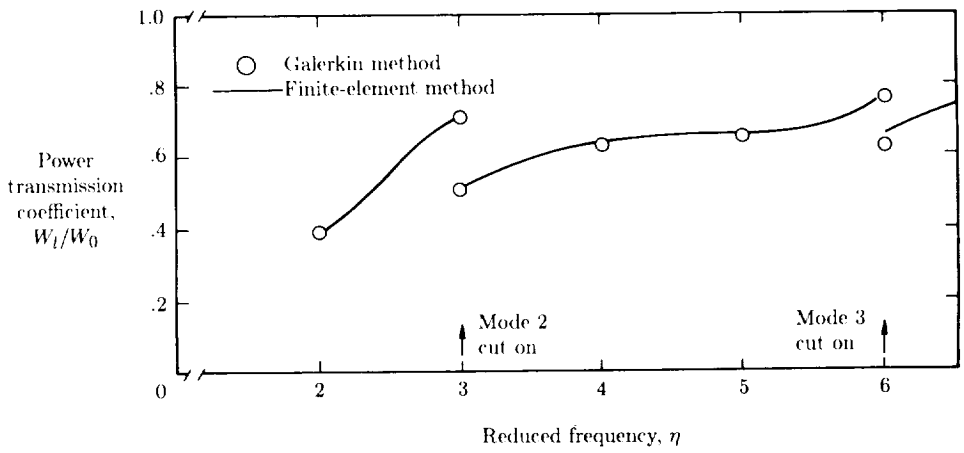

Figure 12. Variation of power transmission coefficient with frequency. $A = 0.72 + i0.42$. *(From ref. 52.)*

this discussion we limit attention entirely to the inlet radiation problem, in which propagation and radiation occur through an inlet flow field (possibly absent). We choose not to examine problems in which propagation and radiation occur through a jet, with the resulting considerations of shear layers.

Radiation from a piston in a plane wall (ref. 112) modeled using the Rayleigh integral and based on the knowledge of the velocity distribution on the piston is the classic technique for calculation of the radiation pattern of a flanged duct. At a duct termination the velocity distribution on the conceptual piston is determined by the acoustic field in the duct. In the textbook case at low frequency, the velocity distribution is assumed to be uniform and the radiation impedance is computed, providing a mechanism for connecting the duct propagation (incident and reflected plane waves) to the radiated field. Levine and Schwinger (ref. 113) considered radiation from an unbaffled open-end pipe using the Wiener-Hopf method. The duct propagation and radiation is treated as a coupled system, and both the radiation pattern and the reflection and transmission coefficients for the duct modes can be calculated. This Levine and Schwinger formulation has been widely used, but as in the case of the Rayleigh integral for the baffled termination, it is limited to the situation when no inlet flow is present.

In order to model rigorously the radiation process when an inlet flow is present, it is appropriate to use the finite-element method. This modeling method, in contrast to the finite-difference method, has the advantage of being readily adaptable to the complex geometry of a turbofan inlet.

When the finite-element method is used, propagation in the duct and radiation to the far field are included in one model. It is assumed that the inlet flow field is irrotational. The appropriate field equations are then equations (9) and (11). Equation (10) is used to compute the local speed of sound from the mean flow velocity potential. Equations (9) and (11) can be combined in a single "wave-like" equation in the acoustic velocity potential, this equation requiring as input data the

mean flow velocity potential, derivatives of the velocity potential, and the local speed of sound.

Two different finite-element models have been developed. The first to appear was developed in references 114 and 115 and is an extension of the finite-element model for duct propagation discussed in references 108 and 109. As noted previously, their field equation in the acoustic velocity potential is a direct combination of equations (9) and (11). A Galerkin method is used to formulate the problem and integration by parts is used to introduce the natural boundary conditions on the duct walls and what amounts to a radiation condition on a boundary outside the duct. The source is introduced through use of a forced boundary condition which specifies acoustic particle velocity on the source plane. The data for their field equation require first and second derivatives of the mean flow velocity potential (velocity and spatial derivatives of velocity). These data are generated by modeling the inlet flow with a boundary-element procedure.

The radiation condition is introduced by representing the acoustic field in terms of a boundary-element method in the region outside a surface exterior to the nacelle, which can be called the matching surface. The procedure is to solve the field equations interior to the matching surface using the finite-element procedure, with the radiation impedance on the matching surface assumed. This allows the computation of the acoustic potential on the matching surface. This is used to generate the exterior acoustic field and, hence, a second version of the radiation impedance. This new impedance is assumed in a new finite-element solution in the interior. The iterative procedure continues until successive finite-element and boundary-element calculations agree on the radiation impedance to some specified accuracy. After the iteration procedure, the acoustic pressure and particle velocity can be obtained by suitable processing of the acoustic velocity potential.

The second finite-element model to appear was reported in references 116 and 117. The approach used was a Galerkin formulation based on the field equations (9) and (11). The authors took advantage of the divergence term in equation (9), which in the Galerkin scheme leads (upon use of the divergence theorem) to introduction of natural boundary conditions and to the elimination of the requirement in the input data for the specification of mean flow velocity spatial derivatives. This makes it attractive to compute the mean flow field from a velocity-potential formulation with a finite-element representation on the same mesh as that used for the acoustic propagation and radiation. The source is modeled in terms of incident and reflected modes, which are matched to the finite-element solution on the source plane.

The radiation to the far field is also modeled with finite elements which have in their shape functions the wave character of the far field of a simple source. These wave-envelope elements allow the use of elements which are very large in the radial direction. With these elements the region between the near field and the far field can be spanned with a relatively small number of elements. At the far-field boundary a simple radiation condition can be imposed. The entire problem is cast in finite-element form so that no iteration is necessary. The solution is carried out with the frontal solution method of reference 84 at a modest cost in computer storage.

Examples of the success of the finite-element modeling of turbofan radiation are shown in figure 13, wherein the finite-element predictions of acoustic radiation from a turbofan engine are compared with the actual radiation patterns measured in a flight test program. The engine was modified to produce a strong tone in the $m = 13$

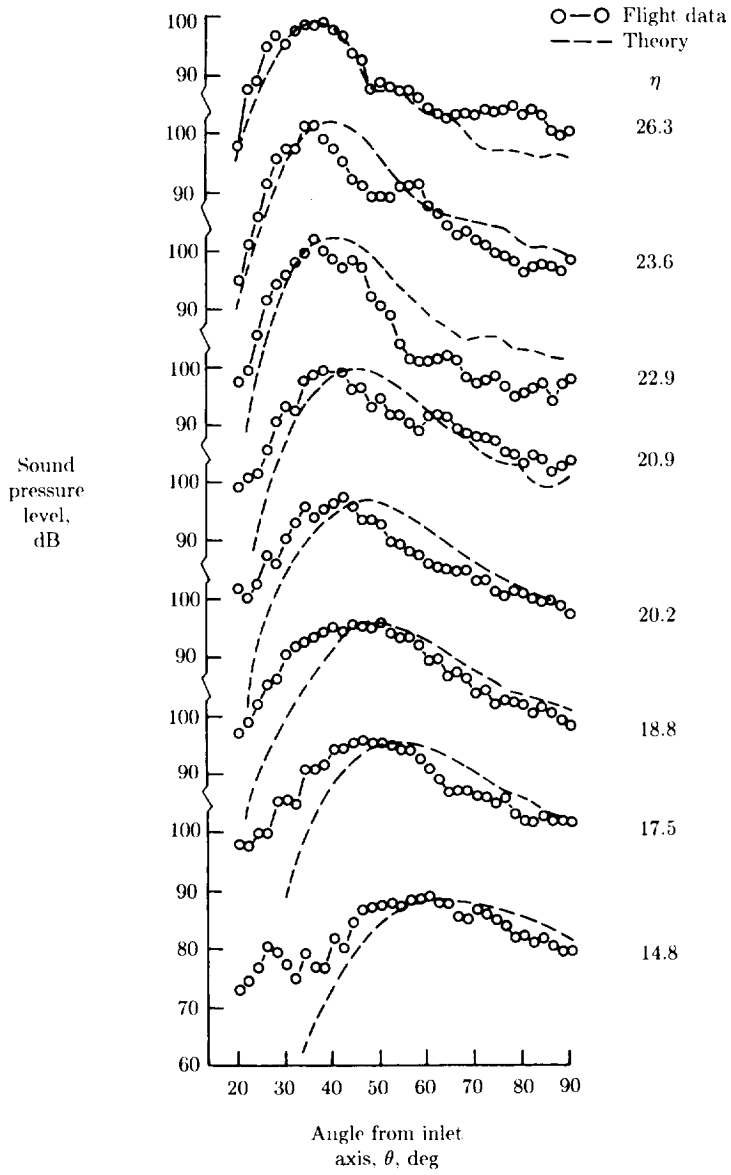

Figure 13. Experimental and computational directivity for JT15D flight inlet including flight effects.

angular mode at frequencies dependent on the engine speed. Figure 13 shows the comparison of theory and measurement for the directivity (SPL vs polar angle from the inlet centerline) for several nondimensional frequencies (based on the duct radius at the throat). The frequencies shown span the range from just barely cut on to well cut on. The agreement is remarkably good, particularly when one considers the complexities of both the modeling scheme and the flyover test procedure.

A ray acoustics model for radiation has been described in references 118 and 119. Only sparse details are available, but it is probable that the major advantage of the method is in its prediction of broadband noise radiation. as opposed to the pure tone radiation for which the finite-element procedure is particularly appropriate.

The complexity of the computation schemes which are required to compute acoustic radiation for lined ducts with interior and exterior flows has led Rice and his co-workers to extend the ideas of modal cutoff ratio to the radiation problem and to derive approximate expressions for the radiation pattern which are functions of the modal cutoff ratios for the duct modes. The starting point is the following expression derived in references 120 and 121 for the mean-square pressure as a function of the polar angle from the inlet axis ψ_o, the modal cutoff ratio β_o, and the frequency $\eta = \omega R/c$ (where R is the duct radius) for radiation from a flanged duct:

$$\overline{P}^2(\psi_o) = \frac{2\sin\psi_o\sqrt{1-1/\beta_o^2}\left(\sin\left\{\eta[\sin\psi_o - (1/\beta_o)]\right\}\right)^2}{\pi\eta[(1/\beta_o^2) - \sin^2\psi_o]^2} \tag{89}$$

This approximation is valid except for the first few radial modes of high-order angular modes. The important feature here is that the approximation to the radiation pattern depends not on the individual modal structure but instead on the cutoff ratio, an implication that all modes with the same cutoff ratio have the same radiation pattern for η being equal. Hence, just as in the suppressor design procedure (refs. 3 and 62 to 65) based on cutoff ratio, it is found that for the simple case of the flanged duct without flow the radiation pattern also depends on cutoff ratio.

Reference 121 combined this idea, the concept of a modal density function (ref. 122), and cutoff ratio biasing function to predict the directivity of broadband (multimodal) fan noise with a substantial degree of success. It was then determined (ref. 6) that the polar angle at which the peak of the radiated field occurs is a function of cutoff ratio. The functional dependence on cutoff ratio can be found for no flow, for inlet flow with no forward-flight effect, and for inlet flow with forward-flight effect. This observation led to the establishment of corrections of equation (89) for the flow effect and additionally for the unflanged duct case (ref. 66).

With this development the entire suppression design procedure can be put in an approximate but vastly simplified context in comparison with the use of the full numerical models. Such a procedure is desirable for preliminary design iterations.

Nonlinear Duct Acoustics

Nonlinear propagation phenomena in ducts present a field of study which is potentially as vast as that of the linear theory discussed to this point. In this section the intention is to address only two problems related to turbofan noise.

Under certain conditions, principally related to the presence of a shock wave system on the fan blades because of supersonic relative tip speeds, acoustic waves are propagated in the duct with a distinctive spectral content. In addition to the interaction tones of the Tyler-Sofrin theory (ref. 5), there exist multiple pure tones which are based on rotor speed rather than on blade passage frequency (refs. 123 to 126). These tones are apparently at least partly due to initially small variations in the shock wave pattern on the rotor because of nonuniformities in the blades. These initially small variations are enhanced because of nonlinear effects related to the shock structure radiated from the blades. In addition, the nonlinear shock structure produces an attenuation in the duct which is not predicted by linear theory (refs. 123 to 126) but which is related to the decay of shock strength away from the rotor face. This decay is enhanced by high subsonic inlet flows and cannot be predicted by linear acoustic theory.

It has been previously noted that in high subsonic inlet flows, the fan tones predicted by the Tyler-Sofrin theory (ref. 5) show an attenuation not predicted by linear theory. This attenuation becomes nearly complete when the inlet flow becomes sonic at the throat. It was also previously noted that linear theory does predict a large increase in the pressure amplitude for acoustic waves incident upon a throat where an approaching flow reaches high subsonic flow. This is illustrated in figure 14 (from ref. 127), wherein the pressure magnitude is plotted against the axial distance for a plane wave approaching a throat with inlet flows of $M = 0.75, 0.85$, and 0.96. The sharp pressure rise for $M = 0.96$ suggests the onset of nonlinear behavior.

A perturbation procedure was used in reference 128 to show that finite-amplitude acoustic modes show nonlinear dispersion and that the characteristic velocity of propagation of acoustic waves becomes dependent on the amplitude of the waves. Since the wave amplitude grows near the throat, as shown in figure 14, the incident waves can stop propagating before the mean flow reaches sonic velocity.

In a series of papers (refs. 129 to 131), the method of matched asymptotic expansions was used to investigate the nonlinear behavior of originally linear planar acoustic waves passing through the throat region of a duct in which the mean flow in the throat is transonic. The formation of acoustic shock waves was demonstrated and, as might be anticipated, it was shown that the nonlinear effects increase with source strength, frequency, and throat Mach number. The shock waves cause a substantial dissipation of energy and are the mechanism by which acoustic choking occurs in the one-dimensional case. The same type of behavior was found in references 132 and 133 with finite-difference solutions of the one-dimensional Euler equations, and good agreement with the matched asymptotic expansion results was also found.

In reference 134 the method of matched asymptotic expansions was extended to two-dimensional propagation. As in the one-dimensional case, shock waves develop in the acoustic field in the near-sonic mean flow in the duct throat. Coupling between acoustic modes induces the nonlinear behavior at lower Mach numbers than in the case of plane-wave propagation. Dispersion plays a major role in this case, whereas it did not in the one-dimensional case.

Much remains to be learned about nonlinear effects, particularly in complicated flows with multimodal propagation. This is a fruitful area for future research.

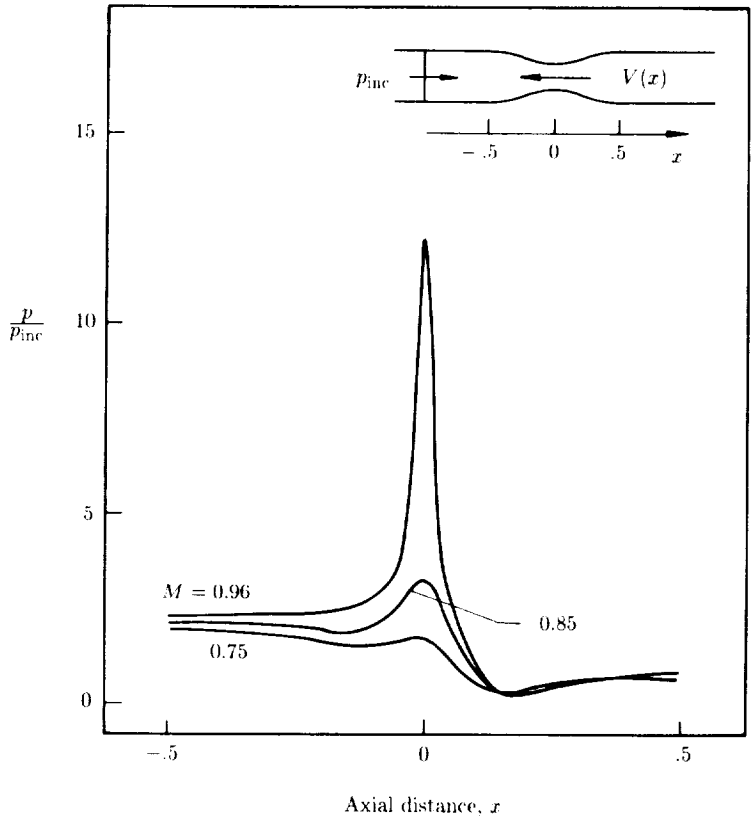

Figure 14. Pressure rise at high subsonic throat for plane wave at inlet Mach numbers of 0.75, 0.85, and 0.96. (From ref. 127.)

References

1. Nayfeh, Ali H.; Kaiser, John E.; and Telionis, Demetri P.: Acoustics of Aircraft Engine-Duct Systems. *AIAA J.*, vol. 13, no. 2, Feb. 1975, pp. 130–153.
2. Eversman, Walter: Energy Flow Criteria for Acoustic Propagation in Ducts With Flow. *J. Acoust. Soc. America*, vol. 49, no. 6, pt. 1, June 1, 1971, pp. 1717–1721.
3. Rice, Edward J.: *Acoustic Liner Optimum Impedance for Spinning Modes With Mode Cut Off Ratio as the Design Criterion.* NASA TM X-73411, 1976.
4. Rschevkin, S. N.: *A Course of Lectures on the Theory of Sound.* MacMillan Co., 1963.
5. Tyler, J. M.; and Sofrin, T. G.: Axial Flow Compressor Noise Studies. *SAE Trans.*, vol. 70, 1962, pp. 309–332.
6. Rice, Edward J.; Heidmann, Marcus F.; and Sofrin, Thomas G.: Modal Propagation Angles in a Cylindrical Duct With Flow and Their Relation to Sound Radiation. AIAA Paper 79-0183, Jan. 1979.
7. Mungur, P.; and Gladwell, G. M. L.: Acoustic Wave Propagation in a Sheared Fluid Contained in a Duct. *J. Sound & Vib.*, vol. 9, no. 1, Jan. 1969, pp. 28–48.
8. Möhring, W.: Über Schallwellen in Scherströmungen. *Fortschritte der Akustik*, DAGA 1976, pp. 543–546.
9. Sivian, L. J.: Sound Propagation in Ducts Lined With Absorbing Materials. *J. Acoust. Soc. America*, vol. 9, no. 2, Oct. 1937, pp. 135–140.
10. Molloy, Charles T.: Propagation of Sound in Lined Ducts. *J. Acoust. Soc. America*, vol. 16, no. 1, July 1944, pp. 31–37.
11. Sabine, Hale J.: The Absorption of Noise in Ventilating Ducts. *J. Acoust. Soc. America*, vol. 12, no. 1, July 1940, pp. 53–57.
12. Morse, Philip M.: The Transmission of Sound Inside Pipes. *J. Acoust. Soc. America*, vol. 11, no. 2, Oct. 1939, pp. 205–210.
13. Morse, Philip M.; and Ingard, K. Uno: *Theoretical Acoustics.* McGraw-Hill Book Co., Inc., c.1968.
14. Cremer, Lothar: Theorie der Luftschall-Dämpfung im Rechteckkanal mit schluckender Wand und das sich dabei ergebende höchste Dämpfungsmass. *Acoustica*, vol. 3, no. 2, 1953, pp. 249–263.
15. Molloy, Charles T.; and Honigman, Esther: Attenuation of Sound in Lined Circular Ducts. *J. Acoust. Soc. America*, vol. 16, no. 4, Apr. 1945, pp. 267–272.
16. Rogers, R.: The Attenuation of Sound in Tubes. *J. Acoust. Soc. America*, vol. 11, no. 4, Apr. 1940, pp. 480–484.
17. Fisher, E.: Attenuation of Sound in Circular Ducts. *J. Acoust. Soc. America*, vol. 17, no. 2, Oct. 1945, pp. 121–122.
18. Rice, Edward J.: Attenuation of Sound in Soft-Walled Circular Ducts. *Aerodynamic Noise*, Univ. of Toronto Press, c.1969, pp. 229–249.
19. Benzakein, M. J.; Kraft, R. E.; and Smith, E. B.: Sound Attenuation in Acoustically Treated Turbomachinery Ducts. ASME Paper 69-WA/GT-11, Nov. 1969.
20. Zorumski, William E.; and Mason, Jean P.: Multiple Eigenvalues of Sound-Absorbing Circular and Annular Ducts. *J. Acoust. Soc. America*, vol. 55, no. 6, June 1974, pp. 1158–1165.
21. Doak, P. E.; and Vaidya, P. G.: Attenuation of Plane Wave and Higher Order Mode Sound Propagation in Lined Ducts. *J. Sound & Vib.*, vol. 12, no. 2, June 1970, pp. 201–224.
22. Christie, D. R. A.: Theoretical Attenuation of Sound in a Lined Duct: Some Computer Calculations. *J. Sound & Vib.*, vol. 17, no. 2, July 22, 1971, pp. 283–286.
23. Vo, P. T.; and Eversman, W.: A Method of Weighted Residuals With Trigonometric Basis Functions for Sound Transmission in Circular Ducts. *J. Sound & Vib.*, vol. 56, no. 2, Jan. 22, 1978, pp. 243–250.
24. Watson, Willie; and Lansing, Donald L.: *A Comparison of Matrix Methods for Calculating Eigenvalues in Acoustically Lined Ducts.* NASA TN D-8186, 1976.
25. Lapin, A. D.: Influence of Motion of the Medium on the Sound Attenuation in a Waveguide Lined With a Sound-Absorbing Material. *Soviet Phys. Acoust.*, vol. 12, no. 4, Apr.–June 1967, pp. 402–404.
26. Eversman, Walter: The Effect of Mach Number on the Tuning of an Acoustic Lining in a Flow Duct. *J. Acoust. Soc. America*, vol. 48, no. 2, pt. 1, Aug. 1970, pp. 425–428.
27. Ko, Sung-Hwan: Sound Attenuation in Lined Rectangular Ducts With Flow and Its Application to the Reduction of Aircraft Engine Noise. *J. Acoust. Soc. America*, vol. 50, no. 6, pt. 1, Dec. 1971, pp. 1418–1432.

28. Ko, S.-H.: Sound Attenuation in Acoustically Lined Circular Ducts in the Presence of Uniform Flow and Shear Flow. *J. Sound & Vib.*, vol. 32, no. 2, May 22, 1972, pp. 193–210.
29. Kraft, R. E.; Motsinger, R. E.; Gauden, W. H.; and Link, J. F.: *Analysis, Design, and Test of Acoustic Treatment in a Laboratory Inlet Duct.* NASA CR-3161, 1979.
30. McCalla, Thomas Richard: *Introduction to Numerical Methods and FORTRAN Programming.* John Wiley & Sons, Inc., c.1967.
31. Bauer, A. B.; and Joshi, M. C.: Classification of Acoustic Modes in a Lined Duct. AIAA-80-1016, June 1980.
32. Eversman, W.: Computation of Axial and Transverse Wave Numbers for Uniform Two-Dimensional Ducts With Flow Using a Numerical Integration Scheme. *J. Sound & Vib.*, vol. 41, no. 2, July 22, 1975, pp. 252–255; Errata, vol. 47, no. 1, July 8, 1976, p. 125.
33. Eversman, W.: Initial Values for the Integration Scheme To Compute the Eigenvalues for Propagation in Ducts. *J. Sound & Vib.*, vol. 50, no. 1, Jan. 8, 1977, pp. 159–162; Errata, vol. 53, no. 4, Aug. 22, 1977, p. 595.
34. Pridmore-Brown, D. C.: Sound Propagation in a Fluid Flowing Through an Attenuating Duct. *J. Fluid Mech.*, vol. 4, pt. 4, Aug. 1958, pp. 393–406.
35. Tack, D. H.; and Lambert, R. F.: Influence of Shear Flow in Sound Attenuation in a Lined Duct. *J. Acoust. Soc. America*, vol. 38, Oct. 1965, pp. 655–666.
36. Kurze, Ulrich J.; and Allen, Clayton H.: Influence of Flow and High Sound Level on the Attenuation in a Lined Duct. *J. Acoust. Soc. America*, vol. 49, no. 5, pt. 2, May 1971, pp. 1643–1654.
37. Kurze, U.: Schallausbreitung im Kanal mit Periodischer Wandstruktur. *Acustica*, vol. 21, no. 2, 1969, pp. 74–85.
38. Goldstein, M.; and Rice, E.: Effect of Shear on Duct Wall Impedance. *J. Sound & Vib.*, vol. 30, no. 1, Sept. 8, 1973, pp. 79–84.
39. Mungur, P.; and Plumblee, H. E.: Propagation and Attenuation of Sound in a Soft-Walled Annular Duct Containing a Sheared Flow. *Basic Aerodynamic Noise Research*, Ira R. Schwartz, ed., NASA SP-207, 1969, pp. 305–327.
40. Eversman, Walter: Effect of Boundary Layer on the Transmission and Attenuation of Sound in an Acoustically Treated Circular Duct. *J. Acoust. Soc. America*, vol. 49, no. 5, pt. 1, May 1971, pp. 1372–1380.
41. Mariano, S.: Effect of Wall Shear Layers on the Sound Attenuation in Acoustically Lined Rectangular Ducts. *J. Sound & Vib.*, vol. 19, no. 3, Dec. 8, 1971, pp. 261–275.
42. Hersh, A. S.; and Catton, I.: Effect of Shear Flow on Sound Propagation in Rectangular Ducts. *J. Acoust. Soc. America*, vol. 50, no. 3, pt. 2, Sept. 1971, pp. 992–1003.
43. Savkar, S. D.: Propagation of Sound in Ducts With Shear Flow. *J. Sound & Vib.*, vol. 19, no. 3, Dec. 8, 1971, pp. 355–372.
44. Unruh, J. F.; and Eversman, W.: The Utility of the Galerkin Method for the Acoustic Transmission in an Attenuating Duct. *J. Sound & Vib.*, vol. 23, no. 2, July 1972, pp. 187–197.
45. Unruh, J. F.; and Eversman, W.: The Transmission of Sound in an Acoustically Treated Rectangular Duct With Boundary Layer. *J. Sound & Vib.*, vol. 25, no. 3, Dec. 1972, pp. 371–382.
46. Eversman, W.; and Astley, R. J.: Acoustic Transmission in Non-Uniform Ducts With Mean Flow. Part I: The Method of Weighted Residuals. *J. Sound & Vib.*, vol. 74, no. 1, Jan. 8, 1981, pp. 89–101.
47. Yurkovich, R. N.: Attenuation of Acoustic Modes in Circular and Annular Ducts in the Presence of Sheared Swirling Flow. AIAA Paper No. 76-498, July 1976.
48. Wynne, G. A.; and Plumblee, H. E.: Calculation of Eigenvalues of the Finite Difference Equations Describing Sound Propagation in a Duct Carrying Sheared Flow. Paper presented at the 79th Meeting of the Acoustical Society of America, Apr. 1970.
49. Dean, L. Wallace, III: Method for Computing Acoustic Mode Properties in Uniformly Treated Ducts With Sheared Flow. Paper presented at the 88th Meeting of the Acoustical Society of America (St. Louis, Missouri), Nov. 1974.
50. Astley, R. J.; and Eversman, W.: A Finite Element Formulation of the Eigenvalue Problem in Lined Ducts With Flow. *J. Sound & Vib.*, vol. 65, no. 1, July 8, 1979, pp. 61–74.
51. Astley, R. J.; and Eversman, W.: The Finite Element Duct Eigenvalue Problem: An Improved Formulation With Hermitian Elements and No-Flow Condensation. *J. Sound & Vib.*, vol. 69, no. 1, Mar. 8, 1980, pp. 13–25.
52. Astley, R. J.; and Eversman, W.: Acoustic Transmission in Non-Uniform Ducts With Mean Flow. Part II: The Finite Element Method. *J. Sound & Vib.*, vol. 74, no. 1, Jan. 8, 1981, pp. 103–121.

53. Astley, R. J.; Walkington, N. J.; and Eversman, W.: Transmission in Flow Ducts With Peripherally Varying Linings. AIAA-80-1015, June 1980.
54. Eversman, Walter; and Beckemeyer, Roy J.: Transmission of Sound in Ducts With Thin Shear Layers – Convergence to the Uniform Flow Case. *J. Acoust. Soc. America*, vol. 52, no. 1, pt. 2, July 1972, pp. 216–220.
55. Eversman, Walter: Approximation for Thin Boundary Layers in the Sheared Flow Duct Transmission Problem. *J. Acoust. Soc. America*, vol. 53, no. 5, May 1973, pp. 1346–1350.
56. Eversman, W.: Representation of a 1/N Power Law Boundary Layer in the Sheared Flow Acoustic Transmission Problem. *J. Sound & Vib.*, vol. 24, no. 4, Oct. 22, 1972, pp. 459–469.
57. Myers, M. K.; and Chuang, S. L.: Uniform Asymptotic Approximations for Duct Acoustic Modes in a Thin Boundary-Layer Flow. *AIAA J.*, vol. 22, no. 9, Sept. 1984, pp. 1234–1241.
58. Rice, Edward J.: Propagation of Waves in an Acoustically Lined Duct With a Mean Flow. *Basic Aerodynamic Noise Research*, Ira R. Schwartz, ed., NASA SP-207, 1969, pp. 345–355.
59. Rice, Edward J.: *Spinning Mode Sound Propagation in Ducts With Acoustic Treatment.* NASA TN D-7913, 1975.
60. Rice, Edward J.: *Spinning Mode Sound Propagation in Ducts With Acoustic Treatment and Sheared Flow.* NASA TM X-71672, 1975.
61. Nayfeh, A. H.; Kaiser, J. E.; and Shaker, B. S.: Effect of Mean-Velocity Profile Shapes on Sound Transmission Through Two-Dimensional Ducts. *J. Sound & Vib.*, vol. 34, no. 3, June 8, 1974, pp. 413–423.
62. Rice, Edward J.: *Attenuation of Sound in Ducts With Acoustic Treatment—A Generalized Approximate Equation.* NASA TM X-71830, 1975.
63. Rice, Edward J.; and Heidelberg, Laurence J.: Comparison of Inlet Suppressor Data With Approximate Theory Based on Cutoff Ratio. AIAA-80-0100, Jan. 1980.
64. Rice, Edward J.: Optimum Wall Impedance for Spinning Modes—A Correlation With Mode Cutoff Ratio. *J. Aircr.*, vol. 16, no. 5, May 1979, pp. 336–343.
65. Rice, Edward J.: Inlet Noise Suppressor Design Method Based Upon the Distribution of Acoustic Power With Mode Cutoff Ratio. *Advances in Engineering Science, Volume 3*, NASA CP-2001, 1976, pp. 883–894.
66. Rice, Edward J.; and Sawdy, David T.: *A Theoretical Approach to Sound Propagation and Radiation for Ducts With Suppressors.* NASA TM-82612, 1981.
67. Morfey, C. L.: Acoustic Energy in Non-Uniform Flows. *J. Sound & Vib.*, vol. 14, no. 2, Jan. 22, 1971, pp. 159–170.
68. Möhring, W.: Energy Flux in Duct Flow. *J. Sound & Vib.*, vol. 18, no. 1, Sept. 8, 1971, pp. 101–109.
69. Möhring, W.: Acoustic Energy Flux in Non-Homogeneous Ducts. AIAA Paper 77-1280, Oct. 1977.
70. Ryshov, O. S.; and Shefter, G. M.: On the Energy of Acoustic Waves Propagating in Moving Media. *J. Appl. Math. & Mech.*, vol. 26, no. 5, 1962, pp. 1293–1309.
71. Candel, S. M.: Acoustic Conservation Principles and an Application to Plane and Modal Propagation in Nozzles and Diffusers. *J. Sound & Vib.*, vol. 41, no. 2, July 22, 1975, pp. 207–232.
72. Eversman, W.: Acoustic Energy in Ducts: Further Observations. *J. Sound & Vib.*, vol. 62, no. 4, Feb. 22, 1979, pp. 517–532.
73. Webster, Arthur Gordon: Acoustical Impedance and the Theory of Horns and of the Phonograph. *Proc. Natl. Acad. Sci.*, vol. 5, no. 1, Jan. 15, 1919, pp. 275–282.
74. Cummings, A.: Acoustics of a Wine Bottle. *J. Sound & Vib.*, vol. 31, no. 3, Dec. 8, 1973, pp. 331–343.
75. Nayfeh, Ali Hasan; and Telionis, Demetri P.: Acoustic Propagation in Ducts With Varying Cross Sections. *J. Acoust. Soc. America*, vol. 54, no. 6, Dec. 1973, pp. 1654–1661.
76. Stevenson, A. F.: Exact and Approximate Equations for Wave Propagation in Acoustic Horns. *J. Appl. Phys.*, vol. 22, no. 12, Dec. 1951, pp. 1461–1463.
77. Zorumski, William E.: *Acoustic Theory of Axisymmetric Multisectioned Ducts.* NASA TR R-419, 1974.
78. Alfredson, R. J.: The Propagation of Sound in a Circular Duct of Continuously Varying Cross-Sectional Area. *J. Sound & Vib.*, vol. 23, no. 4, Aug. 22, 1972, pp. 433–442.
79. Lansing, D. L.; and Zorumski, W. E.: Effects of Wall Admittance Changes on Duct Transmission and Radiation of Sound. *J. Sound & Vib.*, vol. 27, no. 1, Mar. 8, 1973, pp. 85–100.
80. Joshi, M. C.; Kraft, R. E.; and Son, S. Y.: Analysis of Sound Propagation in Annular Ducts With Segmented Treatment and Sheared Flow. AIAA-82-0123, Jan. 1982.
81. Finlayson, Bruce A.: *The Method of Weighted Residuals and Variational Principles.* Academic Press, Inc., 1972.

82. Eversman, W.; Cook, E. L.; and Beckemeyer, R. J.: A Method of Weighted Residuals for the Investigation of Sound Transmission in Non-Uniform Ducts Without Flow. *J. Sound & Vib.*, vol. 38, no. 1, Jan. 1975, pp. 105–123.
83. Kaiser, J. E.; and Nayfeh, A. H.: A Wave-Envelope Technique for Wave Propagation in Nonuniform Ducts. AIAA Paper No. 76-496, July 1976.
84. Irons, Bruce M.: A Frontal Solution Program for Finite Element Analysis. *Int. J. Numerical Methods Eng.*, vol. 2, no. 1, Jan.-Mar. 1970, pp. 5–32.
85. Zienkiewicz, O. C.: *The Finite Element Method.* McGraw-Hill Book Co. (UK) Ltd., c.1977.
86. Bathe, Klaus-Jürgen: *Finite Element Procedures in Engineering Analysis.* Prentice-Hall, Inc., c.1982.
87. Young, Cheng-I James; and Crocker, Malcolm J.: Prediction of Transmission Loss in Mufflers by the Finite-Element Method. *J. Acoust. Soc. America*, vol. 57, no. 1, Jan. 1975, pp. 144–148.
88. Kagawa, Yukio; and Omote, Toshio: Finite-Element Simulation of Acoustic Filters of Arbitrary Profile With Circular Cross Section. *J. Acoust. Soc. America*, vol. 60, no. 5, Nov. 1976, pp. 1003–1013.
89. Kagawa, Y.; Yamabuchi, T.; and Mori, A.: Finite Element Simulation of an Axisymmetric Acoustic Transmission System With a Sound Absorbing Wall. *J. Sound & Vib.*, vol. 53, no. 3, Aug. 8, 1977, pp. 357–374.
90. Craggs, A.: A Finite Element Method for Damped Acoustic Systems: An Application To Evaluate the Performance of Reactive Mufflers. *J. Sound & Vib.*, vol. 48, no. 3, Sept. 8, 1976, pp. 377–392.
91. Craggs, A.: A Finite Element Method for Modelling Dissipative Mufflers With a Locally Reactive Lining. *J. Sound & Vib.*, vol. 54, no. 2, Sept. 22, 1977, pp. 285–296.
92. Tag, I. A.; and Akin, J. E.: Finite Element Solution of Sound Propagation in a Variable Area Duct. AIAA Paper 79-0663, Mar. 1979.
93. Astley, R. J.; and Eversman, W.: A Finite Element Method for Transmission in Non-Uniform Ducts Without Flow: Comparison With the Method of Weighted Residuals. *J. Sound & Vib.*, vol. 57, no. 3, Apr. 8, 1978, pp. 367–388.
94. Baumeister, K. J.: Numerical Techniques in Linear Duct Acoustics – A Status Report. *Trans. ASME, J. Eng. Ind.*, vol. 103, no. 3, Aug. 1981, pp. 270–281.
95. Baumeister, Kenneth J.; Eversman, W.; Astley, R. J.; and White, J. W.: Application of "Steady" State Finite Element and Transient Finite Difference Theory to Sound Propagation in a Variable Duct: A Comparison With Experiment. AIAA-81-2016, Oct. 1981.
96. White, James W.: A General Mapping Procedure for Variable Area Duct Acoustics. AIAA-81-0094, Jan. 1981.
97. Large, J. B.; Wilby, J. F.; Grande, E.; and Andersson, A. O.: The Development of Engineering Practices in Jet, Compressor, and Boundary Layer Noise. *Aerodynamic Noise*, Univ. of Toronto Press, c.1969, pp. 43–67.
98. Chestnutt, David; and Clark, Lorenzo R.: *Noise Reduction by Means of Variable Geometry Inlet Guide Vanes in a Cascade Apparatus.* NASA TM X-2392, 1971.
99. Klujber, F.; Bosch, J. C.; Demetrick, R. W.; and Robb, W. L.: *Investigation of Noise Suppression by Sonic Inlets for Turbofan Engines. Volume I – Program Summary.* NASA CR-121126, 1973.
100. Myers, M. K.: On the Acoustic Boundary Condition in the Presence of Flow. *J. Sound & Vib.*, vol. 71, no. 3, Aug. 8, 1980, pp. 429–434.
101. Davis, Sanford S.; and Johnson, Margaret L.: Propagation of Plane Waves in a Variable Area Duct Carrying a Compressible Subsonic Flow. Paper presented at the 87th Meeting of the Acoustical Society of America (New York, New York), Apr. 1974.
102. King, L. S.; and Karamcheti, K.: Propagation of Plane Waves in Flow Through a Variable Area Duct. AIAA Paper No. 73-1009, Oct. 1973.
103. Huerre, Patrick; and Karamcheti, Krishnamurty: Propagation of Sound Through a Fluid Moving in a Duct of Varying Area. *Interagency Symposium on University Research in Transportation Noise – Proceedings, Volume II*, U.S. Dep. of Transportation, 1973, pp. 397–413.
104. Tam, C. K. W.: Transmission of Spinning Acoustic Modes in a Slightly Non-Uniform Duct. *J. Sound & Vib.*, vol. 18, no. 3, Oct. 8, 1971, pp. 339–351.
105. Nayfeh, A. H.; Telionis, D. P.; and Lekoudis, S. G.: Acoustic Propagation in Ducts With Varying Cross Sections and Sheared Mean Flow. AIAA Paper No. 73-1008, Oct. 1973.
106. Nayfeh, A. H.; Kaiser, J. E.; and Telionis, D. P.: Transmission of Sound Through Annular Ducts of Varying Cross Sections and Sheared Mean Flow. *AIAA J.*, vol. 13, no. 1, Jan. 1975, pp. 60–65.
107. Nayfeh, A. H.; Shaker, B. S.; and Kaiser, J. E.: Transmission of Sound Through Nonuniform Circular Ducts With Compressible Mean Flows. *AIAA J.*, vol. 18, no. 5, May 1980, pp. 515–525.

108. Sigman, R. K.; Majjigi, R. K.; and Zinn, B. T.: Determination of Turbofan Inlet Acoustics Using Finite Elements. *AIAA J.*, vol. 16, no. 11, Nov. 1978, pp. 1139–1145.
109. Majjigi, R. K.; Sigman, R. K.; and Zinn, B. T.: Wave Propagation in Ducts Using the Finite Element Method. AIAA Paper 79-0659, Mar. 1979.
110. Lieblein, S.; and Stockman, N. O.: Compressibility Correction for Internal Flow Solutions. *J. Aircr.*, vol. 9, no. 4, Apr. 1972, pp. 312–313.
111. Abrahamson, A. L.: A Finite Element Algorithm for Sound Propagation in Axisymmetric Ducts Containing Compressible Mean Flow. AIAA Paper 77-1301, Oct. 1977.
112. Pierce, Allan D.: *Acoustics An Introduction to Its Physical Principles and Applications.* McGraw-Hill, Inc., c.1981.
113. Levine, Harold; and Schwinger, Julian: On the Radiation of Sound From an Unflanged Circular Pipe. *Phys. Rev.*, vol. 73, no. 4, Second ser., Feb. 15, 1948, pp. 383–406.
114. Horowitz, S. J.; Sigman, R. K.; and Zinn, B. T.: An Iterative Finite Element-Integral Technique for Predicting Sound Radiation From Turbofan Inlets. AIAA-81-1981, Oct. 1981.
115. Horowitz, S. J.; Sigman, R. K.; and Zinn, B. T.: An Iterative Finite Element-Integral Technique for Predicting Sound Radiation From Turbofan Inlets in Steady Flight. AIAA-82-0124, Jan. 1982.
116. Parrett, A. V.; and Eversman, W.: Wave Envelope and Finite Element Approximations for Turbofan Noise Radiation in Flight. *AIAA J.*, vol. 24, no. 5, May 1986, pp. 753–760.
117. Eversman, W.; Parrett, A. V.; Preisser, J. S.; and Silcox, R. J.: Contributions to the Finite Element Solution of the Fan Noise Radiation Problem. *Trans. ASME, J. Vib., Acoust., Stress & Reliab. Des.*, vol. 107, no. 2, Apr. 1985, pp. 216–223.
118. Kempton, A. J.: Ray Theory To Predict the Propagation of Broadband Fan-Noise. AIAA-80-0968, June 1980.
119. Kempton, A. J.; and Smith, M. G.: Ray-Theory Predictions of the Sound Radiated From Realistic Engine Intakes. AIAA-81-1982, Oct. 1981.
120. Saule, Arthur V.: Modal Structure Inferred From Static Far-Field Noise Directivity. AIAA Paper No. 76-574, July 1976.
121. Rice, E. J.: Multimodal Far-Field Acoustic Radiation Pattern Using Mode Cutoff Ratios. *AIAA J.*, vol. 16, no. 9, Sept. 1978, pp. 906–911.
122. Rice, E. J.: *Modal Density Function and Number of Propagating Modes in Ducts.* NASA TM X-73539, 1976.
123. Pickett, Gordon F.: Prediction of the Spectral Content of Combination Tone Noise. *J. Aircr.*, vol. 9, no. 9, Sept. 1972, pp. 658–663.
124. Morfey, C. L.; and Fisher, M. J.: Shock-Wave Radiation From a Supersonic Ducted Rotor. *Aeronaut. J.*, vol. 74, no. 715, July 1970, pp. 579–585.
125. Hawkings, D.: Multiple Tone Generation by Transonic Compressors. *J. Sound & Vib.*, vol. 17, no. 2, July 22, 1971, pp. 241–250.
126. Mathews, D. C.; and Nagel, R. T.: Inlet Geometry and Axial Mach Number Effects on Fan Noise Propagation. AIAA Paper No. 73-1022, Oct. 1973.
127. Myers, M. K.; and Callegari, A. J.: On the Singular Behavior of Linear Acoustic Theory in Near-Sonic Duct Flows. *J. Sound & Vib.*, vol. 51, no. 4, Apr. 22, 1977, pp. 517–531.
128. Tam, C. K. W.: On Finite Amplitude Spinning Acoustic Modes and Subsonic Choking. *J. Sound & Vib.*, vol. 16, no. 3, June 8, 1971, pp. 393–405.
129. Callegari, A. J.; and Myers, M. K.: Nonlinear Effects on Sound in Nearly Sonic Duct Flows. AIAA Paper 77-1296, Oct. 1977.
130. Callegari, A. J.; and Myers, M. K.: Sound Transmission in Ducts Containing Nearly Choked Flows. AIAA Paper 79-0623, Mar. 1979.
131. Myers, M. K.: Shock Development in Sound Transmitted Through a Nearly Choked Flow. AIAA-81-2012, Oct. 1981.
132. Walkington, N. J.; and Eversman, W.: A Numerical Model of Acoustic Choking. Part I: Shock Free Solutions. *J. Sound & Vib.*, vol. 90, no. 4, Oct. 22, 1983, pp. 509–526.
133. Walkington, N. J.; and Eversman, W.: A Numerical Model of Acoustic Choking. Part II: Shocked Solutions. *J. Sound & Vib.*, vol. 104, no. 1, Jan. 8, 1986, pp. 81–107.
134. Myers, M. K.; and Uenishi, K.: Two Dimensional Nonlinear Analysis of Sound Transmission Through a Near-Sonic Throat Flow. AIAA-84-0497, Jan. 1984.